International Geology Review, Vol. 43, 1999, p. 393–416.

Quantifying the Effects of Metasomatism in Mantle Xenoliths: Constraints from Secondary Chemistry and Mineralogy in Udachnaya Eclogites, Yakutia

VLADIMIR N. SOBOLEV,[1] LAWRENCE A. TAYLOR, GREGORY A. SNYDER,

Planetary Geosciences Institute, Department of Geological Sciences, University of Tennessee, Knoxville, Tennessee 37996

ERIC A. JERDE,

Oak Ridge National Labs, Environmental Sciences Division, Mail Stop 6038, Oak Ridge, Tennessee 37830

CLIVE R. NEAL,

Department of Civil Engineering and Geological Sciences, University of Notre Dame, Indiana 46556

AND NIKOLAI V. SOBOLEV

Institute of Mineralogy and Petrography, Siberian Branch, Russian Academy of Sciences, 630309 Novosibirsk, Russia

Abstract

In mantle xenoliths, metasomatism is recorded by compositional variations within and between minerals, and by the introduction of secondary minerals. However, metasomatism has not been quantitatively evaluated as a process with respect to the fluid composition involved. Diamondiferous eclogites from the Udachnaya kimberlite provide a unique suite of samples that allow a semi-quantitative estimation of metasomatic fluid composition.

The basis of our analysis involves comparison of reconstructed whole-rock compositions with measured whole-rock analyses. Primary minerals in these samples are relatively homogeneous, and permit the use of modal analyses and mineral chemistry for reconstruction of "pristine" whole-rock compositions. The metasomatic overprint, which is similar in all samples studied, has produced depletions in SiO_2, Na_2O, and FeO and enrichments in TiO_2, K_2O, MgO, and LREE. Secondary minerals from the samples are interpreted as the direct result of metasomatism (i.e., typical metasomatic minerals such as phlogopite, amphibole, djerfisherite, and sodalite are present in these xenoliths).

Enrichment/depletion signatures demonstrate that the major metasomatic source for Udachnaya eclogites was not derived from the host kimberlite. These metasomatic agents appear to have been more enriched in TiO_2, K_2O, Cl, FeO, and LREE than are kimberlites, and may have contained significant amounts of F, CO_2, and H_2O. The high Ca contents of two samples are interpreted to be the product of metasomatism by a carbonatite-like fluid.

Introduction

MANTLE XENOLITHS brought to the surface provide us with unique information about the deep interior of the Earth. However, such xenoliths always possess a certain degree of alteration as a result of undergoing a wide variety of processes at different temperatures and pressures in the mantle, in transit, and in the crust. Metasomatism within the mantle is one of the processes that overprints primary rock compositions, leading to the alteration and modification of the constituent minerals (cryptic metasomatism) and/or crystallization of new phases (modal metasomatism). However, in almost all cases, effects from these two types of metasomatic processes occur together in a rock, making it difficult to address the nature and composition of metasomatic fluids that were operative in the upper mantle. Understanding the nature of the metasomatizing agent can lead to a better understanding of mantle processes.

Mantle metasomatism is very complex and has

[1]Also at the Institute of Mineralogy and Petrography, Siberian Branch, Russian Academy of Sciences, 630309 Novosibirsk, Russia.

been used as a panacea for many chemical and petrological problems relating to the genesis of mantle xenoliths. Textural relationships, mineralogy, and chemistry of primary and secondary minerals in mantle xenoliths may retain signatures of the metasomatic fluids. Studying secondary minerals and whole-rock chemistry allows one to determine the nature of the fluids, whereas textural relationships between primary and secondary minerals may lead to the unraveling of different stages of metasomatic events. In a detailed study of phlogopite- and richterite-bearing peridotites from the Kimberley pipes, Erlank et al. (1987) proposed a sequence of metasomatic grades for peridotites, from garnet peridotites to K-richterite-phlogopite peridotites. The K-richterite-phlogopite peridotites are considered to represent the end products of upper-mantle metasomatic processes involving H_2O-rich fluids charged with potassium. A similar origin was proposed for MARID (mica-amphibole-rutile-ilmenite-diopside)-suite nodules (Erlank et al., 1987), although in earlier studies, these nodules were thought to be derived from a kimberlitic magma under oxidizing conditions (Dawson and Smith, 1977; Jones et al., 1982; Kramers et al., 1983).

Studies of fluids trapped in micro-inclusions in Indian, African, and Yakutian diamonds have demonstrated the existence of mantle fluids with wide ranges in compositions, from hydrous fluids rich in SiO_2, Al_2O_3, K_2O, and H_2O, to carbonatitic fluids rich in CaO, FeO, MgO, K_2O, and carbonates (Shrauder and Navon, 1994; Shrauder et al., 1994). Carbonatitic and hydrous fluids may exist at 45 kbar and 1100°C and the range of compositions between the two end members (hydrous and carbonatitic) may have been created by: (1) melting induced by heating of phlogopite-carbonate-peridotite or by introducing hydrous fluid into carbonate-peridotite; (2) mixing of carbonatitic and hydrous fluids; or (3) fractional crystallization during cooling of a water-rich carbonatitic fluid (Shrauder and Navon, 1994). Unfortunately, fluid inclusions in diamonds, as well as diamondiferous mantle xenoliths (<1% of all xenoliths in kimberlites; N. V. Sobolev and N. P. Pokhilenko, pers. comm.), are rare. Studying whole-rock compositions and secondary minerals represents an approach in determining the nature of metasomatism, although it gives only a general idea about fluid compositions. Nonetheless, the use of whole-rock chemistry and reconstructed primary whole-rock compositions obtained from modal analyses and mineral chemistry may allow one to determine the composition of the metasomatic fluid(s). This is only possible when all chemical changes in the rock are the result of modal and not cryptic metasomatism—i.e., primary minerals are chemically homogeneous. An attempt was made by Fraracci (1994) to quantify the metasomatic overprint for eclogite xenoliths from the Mir pipe, Yakutia. Fraracci stated that the consistent enrichment and depletion trends observed for each element indicated a common source of metasomatism for all Mir eclogites, and that this source was similar in composition to a kimberlite magma. However, quantification of the metasomatic overprint was complicated by the imprecision of the modal analyses, as well as mineral zonation present in some samples.

Sobolev et al. (1994b) showed that modally metasomatized eclogites from the Udachnaya kimberlite are unusual in the virtual absence of compositional variations within and between primary minerals. Thus, these rocks represent a unique suite of samples where most if not all chemical changes made by metasomatic fluids lead to the appearance of secondary minerals and not to chemical zonations and intergrain variations in primary phases. This permits one to calculate mineral modes and reconstructed *pristine* whole-rock compositions, and to compare these to measured whole-rock analyses.

This study attempts to quantitatively determine the composition of fluids responsible for metasomatic changes in mantle xenoliths, particularly eclogites from the Udachnaya kimberlite pipe. We compare measured whole-rock analyses to reconstructed whole-rock compositions (e.g., $Wr_{measr} - Wr_{reconstr}$ = metasomatism; Fraracci, 1994) in order to discern the nature of the metasomatic fluids. A total of 10 eclogites from the Udachnaya kimberlite of the Yakutian diamondiferous province (Fig. 1) were studied for this purpose. The eclogites were obtained from different horizons of the Udachnaya mine and are relatively fresh. A key assumption is that weathering does not contribute significantly to the alteration of the samples, i.e., that alteration present in these samples is due solely to metasomatic modification of the primary rocks. Although this assumption is an oversimplification, it allows us to

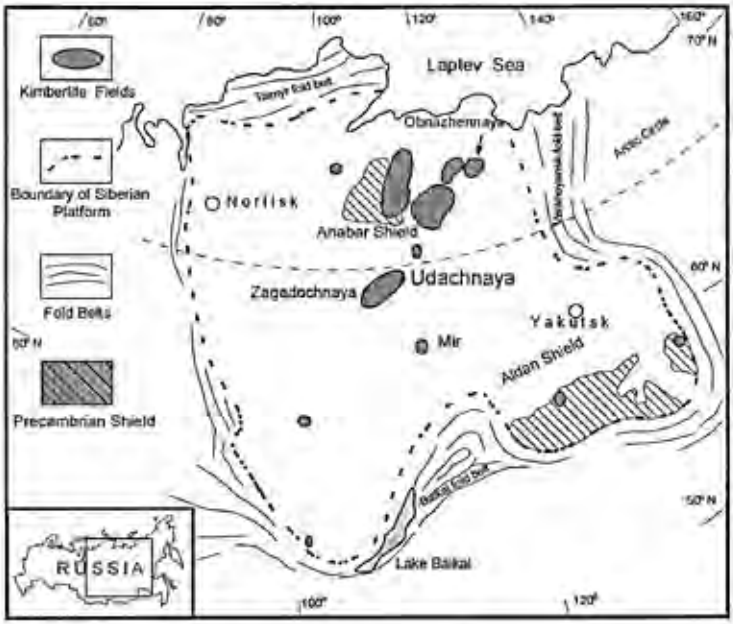

FIG. 1. Simplified geologic map of the Siberian craton.

set constraints on the hypothesized metasomatizing agent that would otherwise be impossible to determine. This assumption is supported by the relative freshness of the host kimberlite (e.g., Kimberlites of Yakutia, Field Guide Book, 1995), and the included xenoliths.

Analytical Techniques

An approximately 30 to 40 mg split of whole-rock powder (representative sample crushed and quartiled) was used for whole-rock analyses, and fused beads were made according to the general procedure of Jezek et al. (1978). Fused-bead analyses were used because there were not sufficient samples for all xenoliths to perform XRF on each sample. It has been shown that the fused-bead technique is a reliable method for obtaining major- and minor-element chemical compositions for small samples (Schuraytz and Ryder, 1990). The electron microprobe (EMP) data on primary minerals were reported by Sobolev et al. (1994b). Major elements were analyzed on a four-spectrometer CAMECA SX-50 electron microprobe at the University of Tennessee. The major-element, bulk-rock compositions were determined by fusing representative portions of samples on a Mo-strip in nitrogen and analyzing the resulting glass by EMP. The accelerating voltage was 15 keV with beam current of 15 nA. The beam size was 20 μm, with a counting time of 20 seconds. All data were corrected using ZAF(PAP) procedures.

Rare-earth-element (REE) analyses of garnet and clinopyroxene were made on individual mineral grains with a modified CAMECA IMS-3f ion microprobe (SIMS) at Washington University. Details of the analytical procedure are given in Zinner and Crozaz (1986) and Lundberg et al. (1988; 1990). The SIMS data on these eclogites were reported previously (Jerde et al., 1993; Sobolev et al., 1994b; Snyder et al., 1997a).

Whole-rock chemistry of the eclogite samples was determined by INAA and EMP. A suite of trace elements was analyzed in whole-rock

splits by instrumental neutron activation (INA). Samples were generally 75 to 100 g in mass and were broken up and crushed in an alumina mortar to <1 mm fragments. The entire mass was then mixed and quartiled to achieve a homogeneous split. Approximately 175 mg of each sample was placed in a polyethylene vial and irradiated in the High Flux Isotope Reactor (HFIR) facility at the Oak Ridge National Laboratory (ORNL). Irradiation was for 9.5 minutes at a flux of 4.5×10^{13} n × $cm^{-2} \times s^{-1}$. After irradiation, the samples were counted using high-purity (intrinsic) germanium detectors and Canberra gamma counting systems connected to a microcomputer (also at the HFIR facility at ORNL). Four counts were made for each sample, at times of approximately 6 hours, 24 hours, 6 days, and 24 days after irradiation, in order to facilitate detection of species with widely ranging half-lives. Counting times were for approximately 1k, 6k, 20k, and 40k seconds for each sample in the four counts, respectively. Comparator standards consisted of solutions of known composition pipetted onto SiO_2 powder and dried. Such standards have an advantage over standard-rock powders in that gamma-ray interferences can be reduced by selection of the elements present in each standard. USGS standard rocks BHVO-1, G-2, W-2, and SCo-1 were run as controls. Peak areas were determined using the ACCUSPEC software provided by Canberra, and data reduced utilizing the methods outlined by Baedecker and Grossman (1989); the elements Fe, Mn, Ca, Na, K, Sc, Cr, Co, Ni, Ga, Rb, Sr, Zr, Cs, Ba, La, Ce, Nd, Sm, Eu, Tb, Dy, Yb, Lu, Hf, Ta, Th, and U are routinely determined. Estimated uncertainties are based on a combination of counting statistics and results for the standard rocks, and are generally less than ±5% relative. Exceptions exist (e.g., Zr, Sr, Rb) where the specific elemental isotope does not activate well, is present in low concentrations, or where the activated isotope has large gamma-ray interferences. Uncertainties for these elements are believed to be < ± 20% relative.

Loss on ignition (LOI) on the whole-rock samples was determined by weighing a whole-rock sample into a porcelain boat and then heating the sample in a muffle furnace at 1000°C for 45 min. The boats were then placed in a desiccator and allowed to cool to room temperature. The samples were weighed again, and the differences between the first and second weighings yielded LOI.

REE concentrations of the Udachnaya kimberlite were determined with a FISONS-VG PlasmaQuad II STE Inductively Coupled Plasma Mass Spectrometer at the University of Notre Dame. Crushed splits of samples for ICP-MS analysis were dissolved using standard HF/HNO_3 techniques on a hot plate at 150°C. The resulting solution was evaporated and the residue treated with two 1-2 mL washes of concentrated HNO_3 before being dissolved and analyzed in 2% HNO_3. All acids used were double-distilled, resulting in a full procedural blank generally at the sub-ppt (part per trillion) level. External calibration procedures were used to quantify elements in the unknowns, and these were prepared from SPEX® liquid standards. Internal standards used were As (as the matrix contained no Cl^- and, hence, no ArCl interference on mass 75), Te, and In. All standards were run as unknowns in order to check calibrations, and blanks were periodically run to check for memory effects, which were minimal at worst. Detection limits for REE are in the parts per billion (ppb) range.

Petrography

A suite of 10 eclogites, 4 of which are diamondiferous, was selected for this study. In hand specimen, these eclogites are coarse-grained, generally equigranular, and have garnet to clinopyroxene volume ratios ranging in proportions from 70:30 to 30:70. Sample 73/3 exhibits a higher proportion of garnet (80%), and sample 1/79 contains 15% kyanite.

The 10 eclogite samples studied represent part of an extensive collection of diamondiferous eclogites from the Udachnaya kimberlite pipe, sampled over an extended period of several years. The mineralogy and petrography of these samples have been described in detail by Sobolev et al. (1994b) and Snyder et al. (1997*a*). Clinopyroxenes are subhedral to anhedral and dark green to pale green in color; they are metasomatically altered to different degrees in all cases. Clinopyroxenes are generally interstitial, occurring between garnet grains, and 1 to 9 mm in longest dimension. They are green to pale-green and in many cases colorless in plane light. In general, clinopyroxenes are more altered than garnet grains of equal size. Some of the clinopyroxenes

have "crinkled" or spongy" reaction rims consisting of fine-grained (50 to 100 μm) clinopyroxenes surrounding the unaltered cores. These reaction rims are similar to the spongy clinopyroxene texture described by Donaldson (1978) and are considered to be a result of metasomatism (Jin and Taylor, 1987; Taylor and Neal, 1989; Beard et al., 1996; Snyder et al., 1997b). In hand specimens, garnets are anhedral and rounded and range from orange to pale orange in color. Garnets have a size range from 0.2 to 8 mm, and the majority are fractured. Alteration rims are common, consisting of phlogopite, amphibole, serpentine, and glass. Full petrographic descriptions and modal mineralogy of the eclogites are given in Sobolev et al. (1994a, 1994b). Note that hereafter, the terms "altered" and "alteration" refer to metasomatic alteration produced by reaction between the primary mineral phase and the metasomatizing agent.

Udachnaya eclogites contain a distinct assemblage of secondary minerals (Table 1). They occur along boundaries (e.g., phlogopite as alteration rim around garnets), as groundmass, and in veins and fractures (e.g., pyroxene, serpentine, and calcite). In general, grain size does not exceed 100 to 200 μm except for sample 41/3, which contains large (1 to 2 mm) books of phlogopite, concentrated in one part of the sample.

Secondary minerals for each sample are shown in Table 1. Note that eclogites 25/84 and 281/84 contain only serpentine as a secondary phase. Serpentine is present in another four samples (Table 1 and Fig. 2A) mainly as fine-grained (10 to 30 μm) material comprising the groundmass. Pyroxene is a common secondary phase (Figs. 2B and D), and it occurs in six eclogites as "crinkled" and "spongy" rims and a fine-grained (<20 μm) groundmass phase. Amphibole as a product of primary clinopyroxene breakdown also is present in some samples. It occurs in alteration rims around garnets (along with phlogopite; Fig. 2B) and as single grains 30 to 50 μm in size. Other minerals, including sulfides, calcite, sodalite, spinel, schorlomite, anhydrite, and celesite are present as fine-grained (5 to 40 μm) material in the groundmass, and in alteration rims around garnets (e.g., schorlomite).

Amphibole, glass, and K-feldspar are present in alteration rims in sample 5/91. All these secondary minerals are fine-grained (<10 μm) and are not distinguishable in practice with the petrographic microscope. These minerals were identified using energy-dispersive analyses (EDS) on the EMP. Sodalite, secondary pyroxene, and calcite also are present in this sample and can be optically identified.

Secondary Mineral Chemistry

Udachnaya eclogites are characterized by the virtual absence of compositional zoning (Sobolev et al., 1994b), in contrast to eclogites from other Yakutian localities (e.g., Mir kimberlite; Beard et al., 1996) and from eclogites worldwide. Although primary garnet and clinopyroxene compositions exhibit significant variations between samples, there are no substantial core-to-rim variations. Only samples 25/84 and 281/84 exhibit intergrain variation (e.g., within individual grains or between grains in a sample) in both garnet and clinopyroxene. Detailed descriptions of the primary mineral chemistry are given in Jerde et al. (1993), Sobolev et al. (1994b), and Snyder et al. (1997a) and will not be presented here.

Representative major-element compositions of secondary minerals are presented in Table 2. It should be noted that, because of the grain size and degree of alteration, it was not possible to perform a complete wavelength-dispersive (WDS) analysis of all secondary minerals. For such minerals, the energy-dispersive mode (EDS) was used to aid in identification.

Phlogopite is present in five samples (Table 1) and does not exhibit significant intergrain compositional variation, with the exception of samples 236/79 and 41/3 (Table 2). Eclogite 236/79 displays significant variations in TiO_2 (0.99 to 2.43 wt%), Al_2O_3 (13.5 to 15.9 wt%), and FeO (5.73 to 7.03 wt%), whereas TiO_2 in sample 41/3 also varies, albeit less dramatically (3.44 to 4.38 wt%).

Amphiboles are present in six eclogites (Table 2). They exhibit intergrain compositional variations in samples 1/79 (e.g., 7.95 to 10.4 wt% Al_2O_3, 12.8 to 15.3 wt% CaO) and 73/3 (7.83 to 12.2 wt% FeO, 12.1 to 16.6 wt% MgO), and are iron-rich in samples 1/79 and 41/3 (12 to 14 wt% FeO). Eclogites 5/91, 51/3, and 237/89 contain amphibole less enriched in FeO (7.71 to 8.97 wt%).

Secondary clinopyroxenes are abundant and their compositions are significantly different from those that are primary. Relative to primary clino-

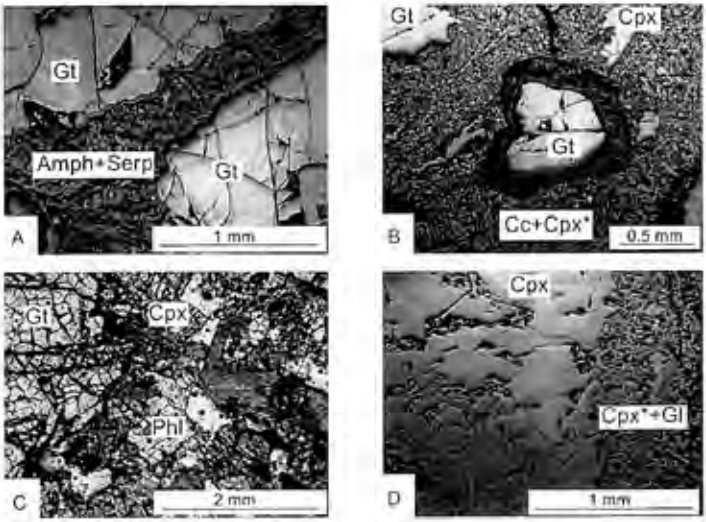

FIG. 2. Secondary minerals in Udachnaya eclogites. A, Amphibole and serpentine in sample 1/79. B, Garnet with alteration rim and secondary clinopyroxene in sample 35/1. C, Crystals of phlogopite in 41/3. D, Secondary clinopyroxene + glass in 5/91.

TABLE 1. Secondary Minerals Observed in the Udachnaya Eclogites[1]

Sample	Secondary minerals
1/79	Amphibole, calcite
5/91	Plagioclase, pyroxene, amphibole, glass, sulfide, calcite, pyrrhotite, chalcopyrite, K-feldspar
25/84	Serpentine
35/1	Pyroxene, schorlomite (Ti-andradite), calcite
41/3	Phlogopite, amphibole, serpentine, pyroxene, spinel, celsian, apatite, calcite, chalcocite
51/3	Phlogopite, amphibole, sekaïte, pyroxene (diopside, aegirine), unidentified P-phase, glass, chalcopyrite, pyrrhotite, djerfisherite, pentlandite
73/3	Phlogopite, Cl-serpentine?, amphibole, pyroxene, pyrite, baddeleyite
256/79	Phlogopite, serpentine, pyroxene, spinel, calcite
237/89	Phlogopite, amphibole, barite, anhydrite, serpentine, calcite
281/81	Serpentine

[1]Silicates = phlogopite; amphibole; serpentine; feldspar; pyroxene; schorlomite (Ti-andradite); and sekaïte. Sulfides = pyrite; pyrrhotite; djerfisherite; pentlandite; chalcopyrite; chalcocite; and heazlewoodite. Other = calcite; anhydrite; apatite; celsian; barite, and spinel.

pyroxenes, they contain less Na (1 to 4 wt% versus 4 to 6 wt% Na_2O) and Al (3 to 7 wt% versus 7 to 9 wt% Al_2O_3), and more Mg (12 to 16 wt% versus 9 to 11 wt% MgO) than coexisting primary clinopyroxenes. However, the Mg#s of the primary and secondary clinopyroxenes are similar (Table 2).

Interstitial sulfides are present in samples 5/91, 41/3, 51/3, and 73/3 (Table 2). They are not abundant and occur as single grains in the groundmass and along fractures. Eclogite 51/3 contains the most abundant sulfide assemblage including chalcopyrite, pyrrhotite, pentlandite, and djerfisherite. Sulfides are fine-grained (10 to

TABLE 2. Major-Element Composition of Secondary Minerals as Determined by EMP

Mineral:	Phlogopite							
Sample:	41/3		51/3	73/3	236/79		237/89	
SiO_2	38.2	38.3	41.1	37.7	40.2	39.4	41.34	
TiO_2	3.44	4.38	0.66	2.63	2.43	0.88	1.07	
Al_2O_3	15.2	14.7	9.88	16.2	13.5	14.7	10.3	
Cr_2O_3	0.16	0.18	<0.03	0.19	0.15	0.08	0.09	
FeO[1]	7.29	7.32	11.9	8.88	5.73	7.03	5.51	
MnO	0.06	<0.03	0.27	0.01	0.01	0.08	0.14	
MgO	20.1	19.8	18.9	19.2	22.7	22.4	25.2	
CaO	0.06	0.03	0.45	0.03	<0.03	<0.03	0.05	
BaO	<0.03	0.15	0.19	0.11	0.07	0.29	0.15	
Na_2O	0.47	0.45	0.04	0.49	0.23	0.27	0.15	
K_2O	10.0	9.96	9.47	9.79	10.7	10.6	10.8	
H_2O	3.98	4.09	3.68	4.03	4.02	3.96	3.77	
F	0.29	0.28	0.58	0.16	0.33	0.40	0.78	
Cl	0.07	0.03	0.05	0.05	0.03	0.06	<0.03	
Total	99.43	99.63	97.12	99.59	100.20	100.05	99.29	
O = F	−0.12	−0.12	−0.25	−0.07	−0.14	−0.17	−0.33	
O = Cl	<0.03	<0.03	<0.03	<0.03	<0.03	<0.03	—	
Total	99.29	99.51	96.86	99.51	100.05	99.87	98.96	
Mg#	83	83	74	79	88	85	89	

Mineral:	Amphibole							
Sample:	1/79		5/91	41/3	51/3	73/3		237/89
SiO_2	37.4	46.9	39.8	39.5	40.7	42.1	39.4	41.5	41.9
TiO_2	0.39	0.29	1.45	1.21	1.57	1.24	0.92	1.62	1.18
Al_2O_3	10.4	7.95	17.3	15.2	15.3	15.5	17.5	15.4	15.2
Cr_2O_3	<0.03	<0.03	0.05	0.07	0.10	<0.03	0.07	0.05	0.08
FeO[1]	11.8	13.5	8.97	12.9	11.1	8.43	12.2	7.83	7.31
MnO	0.17	0.45	0.15	0.27	0.19	0.18	0.23	0.15	0.13
MgO	12.2	13.8	13.7	13.4	13.3	16.7	12.1	16.6	16.9
CaO	15.3	14.1	11.1	11.0	10.4	8.47	10.6	10.9	10.0
Na_2O	1.33	0.93	3.02	1.95	3.03	3.00	3.06	2.88	3.19
K_2O	<0.03	<0.03	2.44	1.90	1.37	0.56	1.18	1.12	0.83
Total	99.13	99.78	98.08	97.30	97.05	96.80	97.22	97.40	97.17
Mg#	65	65	73	65	68	78	64	79	80
Si	7.118	7.810	6.128	6.170	6.374	6.296	6.112	6.226	6.339
Ti	0.044	0.033	0.168	0.142	0.141	0.133	0.107	0.116	0.134
Al	1.841	1.401	3.139	2.798	2.766	2.789	3.199	2.749	2.710
Cr	0.000	0.000	0.006	0.009	0.002	0.012	0.009	0.007	0.010
Fe^{2+}	1.402	1.668	1.155	1.685	1.067	1.436	1.583	0.992	0.926
Mn	0.047	0.057	0.20	0.036	0.023	0.025	0.030	0.019	0.017
Mg	2.733	3.075	3.144	3.120	3.769	3.067	2.798	3.749	3.842
Ca	2.462	2.258	1.831	1.841	1.374	1.724	1.762	1.769	1.621
Na	0.387	0.270	0.603	0.591	1.057	0.909	0.920	0.846	0.936
K	0.000	0.000	0.479	0.379	0.108	0.270	0.234	0.216	0.160
Total	16.114	16.092	16.673	16.769	16.681	16.710	16.754	16.759	16.714

(*continued*)

50 μm) and comprise <1% of the sample. Djerfisherite ($K_6Fe_{20-x}S_{26}Cl$) contains 9 to 10 wt% K_2O and 1.40 wt% Cl (Table 2). Heazlewoodite (Ni_3S_2) is present in sample 73/3, and chalcocite is present in eclogite 41/3 (Table 2).

Calcite, sodalite, spinel, and schorlomite are other minerals that have been analyzed. Calcite is present in six samples and comprises ~30 to 35% of alteration in eclogite 35/1; its composition is given in Table 3. Interstitial sodalite (6 Na[Al-

TABLE 2. (*continued*)

Mineral:	Clinopyroxene and sulfide							
Sample:	5/91	35/1		41/3	51/3		73/3	
SiO_2	54.2	52.40	54.9	52.4	50.2	51.0	52.6	53.1
TiO_2	0.30	0.72	0.56	0.71	0.51	0.34	0.42	0.44
Al_2O_3	3.36	4.64	7.58	5.22	7.87	0.43	3.45	4.19
Cr_2O_3	0.09	0.09	0.09	0.09	0.05	0.07	0.08	0.08
$Fe_2O_3^*$	0.46	2.09	<0.03	1.17	2.84	26.8	1.68	3.00
FeO	4.42	4.45	4.67	7.23	3.76	3.38	4.55	2.29
MnO	0.07	0.18	0.08	0.08	0.21	0.15	0.10	<0.03
MgO	15.4	15.3	13.5	11.9	14.9	1.83	14.9	14.3
CaO	21.2	18.5	14.3	19.0	17.7	3.09	20.1	19.5
Na_2O	1.27	1.66	4.06	2.25	1.57	10.9	1.36	2.38
K_2O	0.03	<0.03	0.03	<0.03	<0.03	<0.03	<0.03	0.03
Total	100.75	99.82	99.77	99.93	99.32	98.0	99.08	99.01
Mg^a	85	81	84	72	81		81	83
Mg^b	83	82		71	79		82	
Si	1.958	1.909	1.966	1.930	1.833	1.998	1.938	1.940
Ti	0.008	0.020	0.015	0.020	0.014	0.010	0.012	0.012
$Al^{(IV)}$	0.042	0.091	0.034	0.070	0.167	0.002	0.062	0.060
$Al^{(VI)}$	0.101	0.109	0.286	0.156	0.171	0.018	0.087	0.121
Cr	0.003	0.003	0.003	0.003	0.001	0.002	0.002	0.002
Fe^{3+}	0.013	0.057	0.000	0.032	0.078	0.790	0.047	0.083
Fe^{2+}	0.133	0.136	0.140	0.223	0.115	0.111	0.140	0.070
Mn	0.002	0.006	0.002	0.002	0.006	0.005	0.003	0.000
Mg	0.829	0.831	0.721	0.653	0.811	0.107	0.818	0.779
Ca	0.821	0.722	0.549	0.750	0.692	0.130	0.793	0.763
Na	0.089	0.117	0.282	0.161	0.111	0.828	0.097	0.169
K	0.001	0.000	0.001	0.000	0.000	0.000	0.000	0.001
Total	4.000	4.000	3.999	4.000	4.000	4.000	4.000	4.000

Mineral:	Sulfides[c]							
Sample:	5/91		41/3	51/3			73/3	
	Po	Cpy	Cc(?)	Cpy	Po	Djf	Py	Hz
S	36.2	33.8	21.9	35.0	31.3	32.5	53.9	27.5
K	<0.03	<0.03	0.41	<0.03	<0.03	9.19	<0.03	<0.03
Ca	0.55	32.4	73.8	33.5	0.40	12.7	0.11	0.09
Ni	0.68	0.64	0.14	1.05	3.19	5.11	3.59	72.9
Fe	62.6	30.4	1.40	31.0	53.7	37.9	44.4	1.55
Cl	n.d.	n.d.	n.d.	n.d.	n.d.	1.40	n.d.	n.d.
Total	100.04	97.29	98.15	100.50	88.56	97.32	102.02	102.06
S	49.7	49.7	36.0	49.9	48.9	45.0	66.2	40.3
K	<0.01	<0.03	0.55	<0.03	<0.03	10.4	<0.03	0.03
Ca	0.38	24.1	61.3	24.0	0.31	8.85	0.07	0.06
Ni	0.51	0.51	0.13	0.81	2.72	3.86	2.41	58.3
Fe	49.3	25.7	1.32	25.3	48.1	30.1	31.3	1.30
Cl	–	–	–	–	–	1.75	–	–

(*continued*)

SiO_4] × 2 NaCl) is found in groundmass and mineral fractures (samples 5/91 and 51/3). Sodalite is similar in composition in samples 5/91 and 51/3, containing 22 to 24 wt% Na_2O and 7.50 to 8.10 wt% Cl (Table 2). Both spinel and schorlomite occur as grains 30 to 50 μm in size in alteration rims around garnets. Schorlomite is present in eclogite 35/1 and spinel is found in samples 41/3 and 236/

TABLE 2. *(continued)*

Mineral:	Sodalite		Spinel		Schorlomite	
Sample:	5/91	51/8[a]	41/3	236/79	35/1	
SiO_2	39.5	36.1 (1)	0.11	0.07	30.1	33.5
TiO_2	<0.03	<0.03 (1)	0.61	0.08	16.9	14.4
Al_2O_3	33.8	31.2 (1)	52.3	64.1	0.34	0.26
Cr_2O_3	0.05	<0.03 (1)	0.17	1.24	<0.03	0.04
FeO	1.09	0.39 (10)	35.3	17.1	13.1	13.2
MnO	<0.03	0.05 (2)	0.34	0.23	4.64	2.80
MgO	<0.03	<0.03	0.90	13.0	0.10	0.12
BaO	0.06	0.05 (2)	n.d.	n.d.	1.97	4.09
CaO	<0.03	<0.03	<0.03	<0.03	32.9	31.7
Na_2O	22.7	24.2 (4)	<0.03	<0.03	0.17	0.42
K_2O	0.14	0.32 (4)	<0.03	<0.03	98.9	99.13
F	<0.03	0.03 (4)	n.d.	n.d.	17	26
Cl	8.10	7.59 (1)	n.d.	n.d.		
Total	105.5	99.89	98.73	99.73		
O = F	–	−0.01				
O = Cl	−1.83	−1.72				
Total	103.67	98.18				
Mg#			38	65		
					Si	2.520	2.722
					Ti	1.064	0.825
					Al	0.034	0.035
					Cr	0.001	0.003
					Fe^{3+}	0.823	0.814
					Fe^{2+}	0.325	0.191
					Mn	0.007	0.008
					Mg	0.246	0.498
					Ca	2.952	2.777
					Na	0.028	0.067
					Total	8.000	8.000

Mineral:	Serpentine				
Sample:	25/84	41/3	73/3		281/84
SiO_2	42.5	34.0	34.7	30.5	35.3
TiO_2	<0.03	0.09	0.16	0.45	0.24
Al_2O_3	0.37	4.05	9.12	13.1	2.30
Cr_2O_3	0.10	<0.03	0.17	<0.03	0.59
FeO	3.90	7.07	9.11	9.39	5.23
MnO	0.34	0.18	<0.03	0.05	0.07
MgO	30.7	35.1	31.1	26.5	39.1
BaO	0.23	0.03	0.14	0.02	<0.03
CaO	<0.03	<0.03	0.07	0.18	<0.03
Na_2O	0.15	<0.03	<0.03	0.08	<0.03
K_2O	0.22	0.03	<0.03	2.20	<0.03
F	n.d.	0.03	0.07	<0.03	n.d.
Cl	n.d.	0.87	0.58	2.15	n.d.
Total	83.51	81.5	85.24	85.44	82.85
O = F	–	−0.01	−0.03	–	–
O = Cl	–	−0.20	−0.13	0.49	–
Total	83.51	81.29	85.08	84.95	82.85
Mg#	86	90	86	83	93

[1]All Fe as FeO.
[2]Fe^{3+} was calculated from EMPA.
[3]Mg/Mg + Fe for secondary clinopyroxenes.
[4]Mg/Mg + Fe for primary clinopyroxenes.
[5]Po = pyrrhotite; Cpy = chalcopyrite; Ce = chalcocite; Djf = djerfisherite; Py = pyrite; Hz = hexatestibite; n.d. = not determined.
[6]Average from three analyses. Unit in parentheses represents one standard unit deviation in terms of the last digit cited.
[7]All Fe as FeO.
[8]Fe^{3+} for schorlomite was calculated from EMPA.

TABLE 3. Major-Element Composition of Glasses, Feldspar, and Calcite[1]

Sample:	1 5/91	2 51/3	3 48-3	4 40-2	Feldspar 5/91	Calcite 35/1	Calcite 236/79
SiO_2	61.1	58.4	52.3	55.3	65.6	<0.03	<0.03
TiO_2	0.04	0.31	0.89	0.48	0.04	<0.03	<0.03
Al_2O_3	21.8	24.4	21.2	21.8	19.5	<0.03	<0.03
Cr_2O_3	<0.03	<0.03	<0.03	0.13	0.03	<0.03	<0.03
FeO[2]	0.44	1.37	4.96	2.35	0.40	0.06	0.06
MnO	0.03	<0.03	0.21	0.25	0.02	<0.03	0.03
MgO	0.98	0.49	1.46	1.46	0.49	0.03	<0.03
CaO	5.12	6.34	4.65	4.44	0.72	58.8	50.2
Na_2O	7.14	7.47	5.99	6.33	0.23	0.00	0.06
K_2O	3.46	0.18	3.16	2.29	14.0	<0.03	<0.03
Total	100.08	98.96	94.76	94.83	101.3	60.0	50.7

[1]Samples 1 and 2 are from this study; samples 3 and 4 are from Hunter and Taylor (1982).
[2]All Fe as FeO.

79 (Table 2). Spinel is more Mg- and Cr-rich in eclogite 236/79 (Table 2).

Glass is found in alteration rims around garnets in samples 5/91 and 51/3. Glasses from these two samples are similar in composition with the exception of K_2O contents: 3.46 wt% K_2O in eclogite 5/91 and 0.18 wt% of K_2O in sample 51/3 (Table 3). Glasses from Udachnaya eclogites are compared with those from kimberlite of Fayette County, Pennsylvania (Table 3, data from Hunter and Taylor, 1982). Glasses described by Hunter and Taylor (1982) are more Fe-rich (2.35 and 4.96 wt% FeO) and Ti-rich (0.48 and 0.89 wt% TiO_2) than those from samples 5/91 and 51/3 (0.44 and 1.37 wt% FeO, 0.04 and 0.31 wt% TiO_2).

Serpentine is present in samples 25/84, 41/3, 73/3, and 281/84. All serpentines contain Cl in the amounts of 0.55 to 2.15 wt% (analyzed by EMP), which is unusual for this mineral. Minor amounts of anhydrite, barite (237/89), celestite, and apatite (41/3) are present as single grains 10 to 20 μm in size in the groundmass.

Quantifying the Effects of Metasomatism

The Udachnaya eclogites are unusual in the virtual absence of compositonal variations within and between primary minerals. This is important as the quantification of the metasomatic overprint is always complicated by the imprecision of modal analyses and mineral zonation present in some samples. The homogeneity and zoning profiles of eclogite minerals would not be affected by the rapid infiltration of kimberlitic fluids during eruption (Qi et al., 1994; Taylor et al., 1996). The eruption event and consequent cooling are extremely rapid in terms of geologic time, and therefore any chemical changes in the composition of the primary minerals (i.e., zonation) during that time would be insignificant. All Udachnaya eclogite xenoliths from the current study appear to be homogeneous, as shown by Sobolev et al. (1994b). This *rules out* cryptic metasomatism during kimberlite eruption. Thus, most if not all chemical changes made by the metasomatic fluids lead to the appearance of secondary minerals. This makes the precision of calculated mineral modes high, and permits one to reconstruct *pristine* whole-rock compositions and to compare these to measured whole-rock analyses.

We have derived a series of equations to quantify the effects of metasomatism, assuming that the alteration that is seen is from mantle processes alone. The derivation of these equations is presented in Sobolev (1997) and the Appendix. Taking into account the primary mineralogy, mineral chemistry, and fluid chemistry, the equations reduce to the difference between the original (calculated) whole-rock composition (C^i_{OWR}) and that of the altered whole-rock (C^i_{AWR}). This difference is presented as Δ^i_m, which is the numerical expression of the influence of the metasomatic fluid (C^i_{MF}).

TABLE 4. Measured Whole-Rock (MWR) and Primary Whole-Rock (PWR) Compositions

	1/79		5/91		23/84		35/1		41/3	
Sample:	PWR	MWR	PWR	MWR	PWR	MWR	PWR	MWR	PWR	MWR
SiO_2	46.8	36.9	48.7	45.5	48.2	41.2	48.6	38.4	44.2	38.3
TiO_2	0.15	0.29	0.22	0.48	0.26	0.27	0.49	0.51	0.41	0.76
Al_2O_3	25.8	17.9	17.5	14.8	11.8	10.7	15.0	5.73	16.2	15.0
Cr_2O_3	0.02	0.04	0.05	0.06	0.54	0.55	0.06	0.06	0.04	0.06
FeO	7.57	5.80	8.66	7.76	6.60	6.25	10.5	7.27	15.9	13.6
MnO	0.14	0.30	0.17	0.23	0.27	0.25	0.19	0.11	0.28	0.30
MgO	6.62	20.0	8.48	12.3	16.8	24.3	13.4	14.5	8.34	15.1
CaO	8.60	7.47	11.4	10.5	14.2	8.37	8.50	19.9	11.83	8.40
Na_2O	3.71	0.47	4.04	1.84	0.95	0.53	3.18	1.82	1.71	0.77
K_2O	0.01	0.09	0.04	1.78	0.01	0.32	0.04	0.34	0.06	0.95
LOI%		10.8		4.80		7.35		11.4		6.82
La	0.02	4.60	0.17	5.13	1.57	8.34	0.43	5.66	0.43	14.1
Ce	0.20	7.72	2.40	12.1	6.41	20.7	2.14	11.9	1.42	26.0
Nd	1.45	3.40	6.39	10.6	5.75	8.07	1.75	4.30	2.06	8.17
Sm	1.06	1.23	2.24	2.94	1.66	2.26	0.53	1.32	1.27	1.97
Eu	0.47	0.58	0.81	1.00	0.50	0.80	0.19	0.42	0.56	0.75
Tb	0.34	0.30	0.33	0.40	0.35	0.44	0.27	0.22	0.57	0.46
Tm	0.24	0.32	0.20	0.35	0.22	0.42	0.25	0.54	0.45	0.81
Yb	1.31	1.34	1.23	1.26	1.37	1.83	1.84	1.24	2.96	2.72
Lu	0.29	0.21	0.22	0.21	0.30	0.25	0.32	0.20	0.48	0.43

	51/5		73/3		230/79		237/89		281/84	
Sample:	PWR	MWR	PWR	MWR	PWR	MWR	PWR	MWR	PWR	MWR
SiO_2	47.8	46.5	42.6	40.9	45.6	39.3	47.7	42.6	43.9	36.1
TiO_2	0.40	0.35	0.47	0.51	0.37	0.37	0.29	0.36	0.40	0.55
Al_2O_3	15.9	12.7	18.9	15.5	16.7	15.8	13.9	14.9	12.8	12.8
Cr_2O_3	0.08	0.07	0.10	0.11	0.12	0.15	0.14	0.13	0.07	0.05
FeO	11.0	8.09	13.3	10.7	8.18	8.13	7.90	8.42	9.08	9.09
MnO	0.20	0.10	0.21	0.17	0.16	0.18	0.17	0.22	0.33	0.30
MgO	14.2	15.1	11.4	16.6	14.8	20.4	15.0	18.0	17.0	26.0
CaO	7.59	9.42	11.6	9.00	12.8	8.41	12.5	9.40	11.8	6.71
Na_2O	2.72	2.32	0.94	0.87	1.15	0.54	1.68	0.91	0.66	0.16
K_2O	0.03	0.85	0.02	0.51	0.00	0.16	0.03	0.55	0.01	0.10
LOI%		3.56		5.27		6.54		4.51		7.20
La	0.46	3.44	0.10	6.94	0.67	4.36	0.43	5.06	0.99	0.01
Ce	1.85	6.99	0.60	12.2	3.45	8.91	1.89	11.6	3.79	23.2
Nd	1.55	3.60	1.58	6.51	3.31	5.40	0.76	5.90	3.45	7.85
Sm	0.54	1.01	1.08	1.40	0.85	1.41	0.60	1.47	1.34	1.96
Eu	0.18	0.34	0.51	0.65	0.30	0.47	0.23	0.54	0.50	0.70
Tb	0.18	0.21	0.23	0.30	0.18	0.20	0.21	0.28	0.44	0.56
Tm	0.25	0.63	0.12	0.26	0.10	0.48	0.11	0.73	0.43	0.86
Yb	1.75	1.85	0.87	0.78	0.44	0.58	0.65	0.96	2.78	3.36
Lu	0.24	0.30	0.14	0.13	0.06	0.10	0.09	0.15	0.48	0.50

Major elements

Bar graphs of absolute Δ'_m for each major-element oxide are shown in Figure 3. It was noted previously that uncertainties in modal abundances obtained from coarse-grained thin sections (with grains >5 mm) are on the order of ±10% (Jerde et al., 1993). These authors also showed that REE patterns for eclogitic assemblages are relatively insensitive to variance in

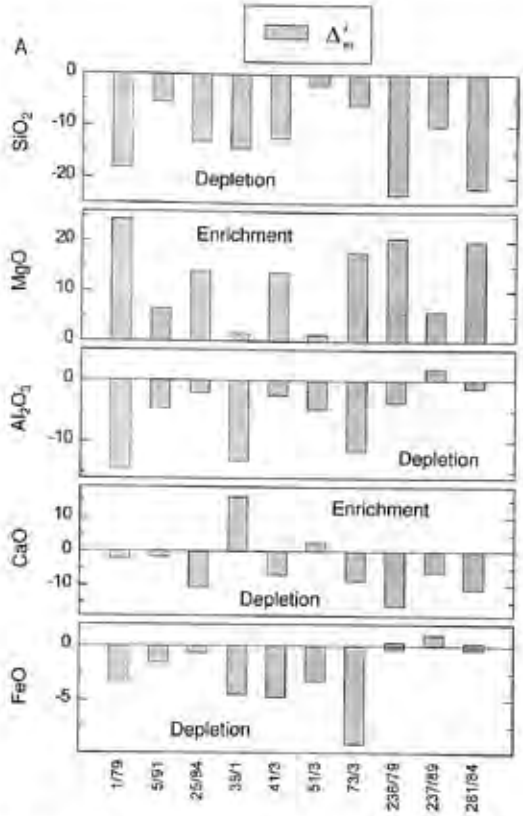

FIG. 3. Absolute Δ^i_m values for the Udachnaya eclogites. X axis is the wt% of the constituent oxides.

mode. However, a 10% error was taken into account. Resultant Δ^i_m values less than this error range were assumed to be indistinguishable from zero and are not indicated on Figure 3. The Δ^i_m values are larger than the values determined by subtracting primary whole-rock (C^i_{PWR}) compositions directly from analyzed whole-rock (C^i_{MWR}) compositions and represent only the suspected addition made by the metasomatic fluid. Some general trends of metasomatic enrichment/depletion can be seen in Figure 3. These trends are reflective of those in Table 4 (primary versus measured whole-rock). There is enrichment in MgO and K_2O with depletion in SiO_2 and Na_2O for all eclogites; Al_2O_3 is depleted in all but eclogite 237/89; TiO_2 is enriched in all but samples 25/84, 35/1, and 236/79 (Fig. 3B).

Table 5 is a numerical expression of the Δ^i_m values used in Figure 3, showing enrichment or depletion of the altered whole-rock composition (C^i_{AWR}) when compared with the original whole-rock composition (C^i_{PWR}). It is important to notice the overall depletion in SiO_2 and enrichment in MgO, which could be interpreted as indicating an influence by the host kimberlite that is characterized by relatively low SiO_2 (23 to 28 wt%) and high MgO (23 to 30 wt%) contents (Table 5). Al_2O_3 does not change significantly in most samples except 1/79 (enriched) and 35/1 (depleted). The overall depletion of CaO should be

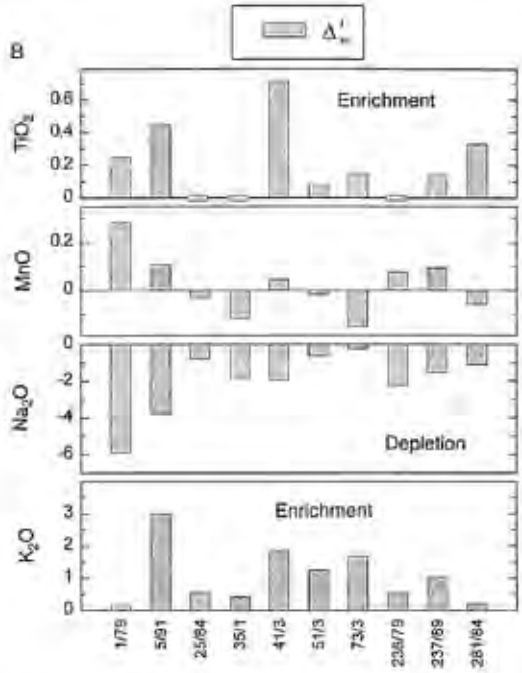

FIG. 3. Continued (caption on facing page).

noted with the notable exception of sample 35/1, where it is strongly enriched. All samples show either depletion or no change in FeO between reconstructed and measured whole-rock compositions. There is no distinctive overall enrichment or depletion for Cr_2O_3 and MnO. All samples are enriched in TiO_2 and K_2O and depleted in Na_2O, which also could be the result of "kimberlite" infiltration metasomatism.

Rare-earth elements

Whole-rock reconstructions using REE data contain valuable signatures of both the primary rock and/or metasomatic fluids. Figure 4 shows the original whole-rock composition (C_{OWR}) for Udachnaya eclogites as compared to the altered whole-rock composition (C'_{AWR}). Delta (Δ'_w) values for REE also are shown in Table 5. Note that all C'_{AWR} patterns are enriched in LREE and MREE relative to C_{OWR} patterns. Some samples show significant enrichment (236/79 and 237/89) and others show depletion (35/1, 41/3 and 73/3) in HREE (C'_{AWR} relative to C_{OWR}). The two Group A eclogites (25/84 and 281/84) exhibit similar C'_{AWR} patterns when compared to C_{OWR} (generally LREE enriched; Figs. 4C and 4G). Sample 1/79 shows the largest enrichment in LREE (over three orders of magnitude; Table 5) from C_{OWR} to C'_{AWR}, whereas eclogite 25/84 possesses the smallest (1.5 orders of magnitude; Table 5). The picture becomes more complicated when comparing HREE abundances. They are depleted in samples 1/79 (HREE approach zero and therefore are not shown in Fig. 4A), 35/1, 41/3, and 73/3. Altered whole-rock compositions are generally enriched in HREE in samples 25/84, 236/79, 237/89, and 281/84.

Secondary minerals as indicators of metasomatism

Cl- and Na-bearing phases. Several samples contain Cl-bearing secondary phases, such as so-

TABLE 5. Absolute and Relative Δ_m Values[1]

	1/79		5/91		2584		35/1		41/3	
Sample:	$\Delta_m(a)$	$\Delta_m(r)$	$\Delta_m(a)$	$\Delta_m(r)$	$\Delta_m(a)$	$\Delta_m(r)$	$\Delta_m(a)$	$\Delta_m(r)$	$\Delta_m(a)$	$\Delta_m(r)$
SiO_2	−18.2	−24.3	−5.45	−10.4	−13.1	−25.8	−14.4	−26.7	−12.3	−26.4
TiO_2	0.25	121	0.45	186	0.02	10.4	0.03	5.80	0.73	180
Al_2O_3	−14.5	−83.3	−4.58	−29.6	−2.07	−26.0	−13.2	−98.9	−2.41	−17.2
Cr_2O_3	0.02	62.0	0.01	30.5	0.02	3.22	0.00	−1.01	0.03	37.5
FeO	−3.23	−65.2	−1.54	−28.1	−0.67	−12.9	−4.52	−49.4	−4.74	−34.7
MnO	0.28	367	0.11	115	−0.03	−17.9	−0.12	−72.4	0.05	20.3
MgO	24.4	364	6.52	82.1	14.0	84.5	1.56	12.2	13.9	159
CaO	−2.06	−20.6	−1.69	−14.6	−10.8	−64.2	16.2	170	−7.07	−55.4
Na_2O	−5.92	−90.3	−3.78	−67.1	−0.79	−61.6	−1.87	−49.1	−1.94	−81.6
K_2O	0.15	659	3.00	5930	0.57	2940	0.42	833	1.85	2300
La	8.38	30000	8.52	3660	12.5	591	7.43	1413	28.2	4715
Ce	15.8	4700	16.7	546	26.8	307	13.9	534	50.7	2673
Nd	3.57	258	7.24	119	4.34	57.5	3.65	180	12.6	535
Sm	0.41	61.1	1.20	82.2	1.13	57.2	1.12	197	1.44	124
Eu	0.21	74.9	0.33	68.9	0.57	106	0.33	176	0.39	83.7
Tb	−0.00	−49.3	0.12	73.0	0.17	59.4	−0.06	−27.9	−0.22	−49.9
Tm	0.15	140	0.26	277	0.37	276.6	0.41	297	0.74	218
Yb	−0.85	−102	0.06	10.3	0.87	102	−0.85	−60.7	−0.51	−22.5
Lu	−0.13	−110	−0.01	−11.8	−0.09	−52.1	−0.18	−72.0	−0.11	−30.0

	51/3		73/3		256/79		237/89		281/81	
Sample:	$\Delta_m(a)$	$\Delta_m(r)$	$\Delta_m(a)$	$\Delta_m(r)$	$\Delta_m(a)$	$\Delta_m(r)$	$\Delta_m(a)$	$\Delta_m(r)$	$\Delta_m(a)$	$\Delta_m(r)$
SiO_2	−2.02	−4.05	−5.98	−12.9	−23.8	−48.7	−10.0	−19.5	−22.1	−46.0
TiO_2	0.08	18.7	0.15	35.2	0.02	4.01	0.14	54.0	0.33	96.0
Al_2O_3	−1.78	−34.3	−11.7	−76.6	−3.60	−25.9	1.96	20.6	−1.24	−12.6
Cr_2O_3	−0.01	−14.2	0.04	39.7	0.10	89.6	−0.03	−22.6	−0.04	−5.12
FeO	−3.27	−34.0	−9.09	−85.7	−0.20	−3.03	1.03	18.1	0.03	0.39
MnO	−0.02	−11.1	−0.15	−97.8	0.08	59.12	0.09	92.9	−0.06	−22.4
MgO	1.33	9.87	17.8	155	20.8	142	5.96	41.7	20.2	119
CaO	2.00	32.1	−8.84	−66.8	−16.2	−111	−6.12	−49.1	−11.3	−80.6
Na_2O	−0.61	−17.6	−0.25	−13.8	−2.25	−137	−1.53	−59.9	−1.12	−124
K_2O	1.25	2980	1.68	3250	0.56	10400	1.01	2428	0.21	1493
La	4.55	775	23.5	13000	13.7	1413	0.17	1378	18.0	1306
Ce	7.85	535	39.9	4266	20.2	410	19.4	714	43.6	833
Nd	3.14	166	16.9	1042	7.74	179	8.19	340	9.90	226
Sm	0.72	120	1.09	120	2.07	233	1.72	261	1.40	94.0
Eu	0.24	125	0.50	122	0.63	220	0.62	293	0.46	93.8
Tb	0.04	26.4	0.22	122	0.06	38.4	0.15	111	0.26	72.3
Tm	0.58	299	0.48	565	1.42	1906	1.22	2012	0.97	296
Yb	0.46	11.8	−0.30	−50.1	0.50	147	0.62	182	1.31	64.2
Lu	0.08	45.14	−0.04	−36.1	0.12	237	0.11	239	0.05	14.1

[1](a) = absolute (r) = relative.

dalite (5/91, 51/3), djerfisherite (51/3), and Cl-rich serpentine (1/79, 41/3, 73/3). This may point to the involvement of Na-Cl–rich metasomatic fluids, although it is conceivable that sodalite and Cl-serpentine could be the result of surface alteration (weathering). However, the occurrence of sodalite along with djerfisherite may, in fact, support a metasomatic origin. According to Godovikov (1983) and Deer et al. (1992), sodalite is not a typical weathering mineral. Spetsius et al. (1985)

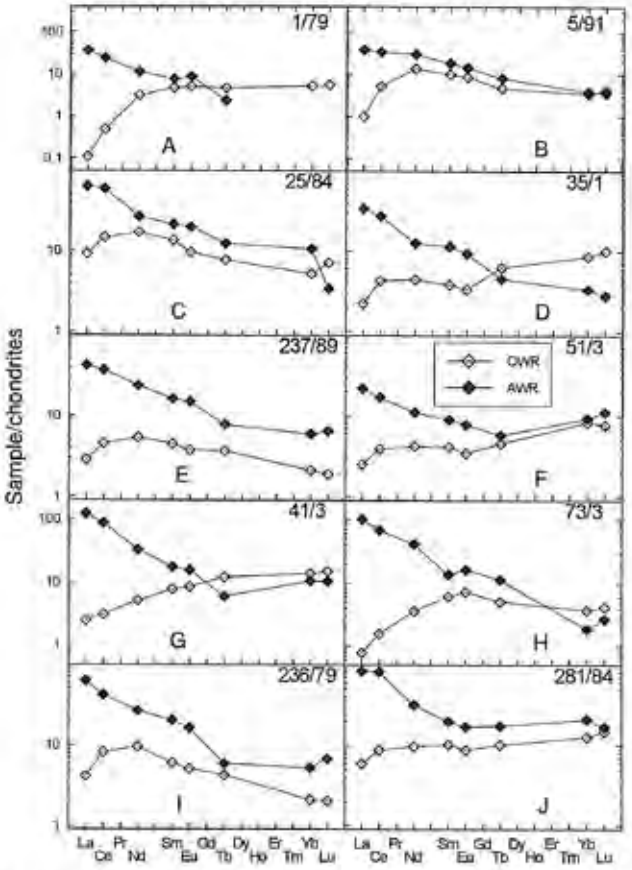

FIG. 4. REE abundances for primary whole-rock (C^{*}_{WR}), measured whole-rock (C_{AWR}), and Udachnaya kimberlite.

studied djerfisherite from several mantle xenoliths (including three eclogites) from the Udachnaya pipe and suggested a metasomatic origin for this mineral. This is in agreement with an earlier conclusion of Bulanova et al. (1982) that djerfisherite ($K_6Fe_{26-x}S_{26}Cl$) originated as a result of alkali metasomatism of primary sulfides (e.g., pyrite and pyrrhotite):

$$26Fe_{1-\delta}S + 6K^{+} + Cl^{-} \rightarrow K_6Fe_{26-x}S_{26}Cl.$$

Goyorov et al. (1984) also found djerfisherite as globular and drop-shaped inclusions in eclogitic clinopyroxene from the Udachnaya kimberlite, and suggested that it was primary and not a result of weathering.

Brenan (1993) stated that Cl and F may be important components of metasomatic fluids. Ayers and Eggler (1995) conducted fluid/melt partitioning experiments at 15 and 20 kbar pressure between synthetic andesite melt and NaCl-H_2O and found that $D^{fluid/melt}$ values range from 0.43 to 1.31 for K, Rb, Sr, La, Sm, Y, Tm, Ti, and Zr. It was stated that the addition of a small amount of NaCl to supercritical H_2O significantly increases the solubility of silicate melt in the fluid. Thus,

the metasomatic agent that affected eclogite 51/1 may have been Na-Cl enriched. However, this is not supported by the fact that the whole-rock analyses show depletion in Na when compared to the primary whole-rock compositions (Table 4). It is possible that Na was released by breakdown of primary omphacite, leading to development of the secondary clinopyroxene, which possessed lesser amounts of Na_2O (5.51 versus 1.57 wt% Na_2O, respectively). Moreover, the amount of released Na was sufficient to form such phases as sodalite and aegirine (10.9 wt% Na_2O), which also are present in eclogite 51/3. Note that eclogite 51/1 possesses the least depletion in Na_2O (2.72 wt% in PWR versus 2.32 wt% in MWR, Table 4), indicating either a Na-enriched metasomatic agent or a unique thermodynamic condition, which would allow Na to stay in the system.

The observed depletion in Na is consistent with the negative pressure effect on the solubility of this component in the stability field of Na-rich clinopyroxenes (Ryabchikov and Kogarko, pers. commun.). According to Ryabchikov (1993) and Ryabchikov et al. (1982), the Na content in metasomatic fluids interacting with Na-bearing clinopyroxene should increase with decreasing pressure, therefore leaching Na from the rock.

Phlogopite. Phlogopite is the most common metasomatic mineral in mantle xenoliths. Erlank et al. (1987) subdivided phlogopite into primary and secondary varieites based upon its appearance in the rock. According to Erlank et al. (1987), primary phlogopites include those that are: (1) in the process of replacing other minerals; (2) forming irregular aggregates with other minerals; or (3) highly deformed. All other phlogopites (e.g., in veins, fractures, alteration rims) are included in the secondary category. Dawson and Smith (1975) also found that primary phlogopites contain less (0.5 to 1.1 wt%) Cr_2O_3 than do their secondary counterparts (>1.1 wt%). Supporting this, Erlank et al. (1987) observed that primary phlogopites from garnet-phlogopite peridotites fall within the range of 0.6 to 1.2 wt% Cr_2O_3, whereas secondary phlogopites from all other peridotite groups (i.e., phlogopite and K-richterite-phlogopite peridotites; Erlank et al., 1987) usually have >1.2 wt% Cr_2O_3 and none <0.6 wt% Cr_2O_3.

All phlogopites from Udachnaya eclogites contain less than 0.2 wt% Cr_2O_3 (Table 2), which is similar to that in MARID (Erlank et al., 1987) rocks. Udachnaya phlogopites also are similar to those in MARIDs in that they span a wide range in TiO_2, from 0.66 to 4.38 wt% TiO_2. The presence of primary metasomatic phlogopite is one more piece of evidence supporting kimberlite-like metasomatic fluids rich in K, Ti, and F.

Phlogopite from sample 41/3 is the only secondary (primary metasomatic) mineral for which the isotopic composition has been determined (Snyder et al., 1997a). They also determined the isotopic composition for sample 108/3 and showed that the abundances of Sr in phlogopite separates are highly variable (109 ppm in 41/3 and 1429 ppm in 108/3). The phlogopite from eclogite 41/3 yields $^{87}Sr/^{86}Sr$, $^{147}Sm/^{144}Nd$, and $^{143}Nd/^{144}Nd$ ratios of 0.7541, 0.0810, and 0.512605, respectively. Snyder et al. (1997a) demonstrated that the Sr whole-rock isotopic composition of all whole rocks is more radiogenic than garnet and clinopyroxene separates. According to these authors, whole-rock isotopic compositions reflect the involvement of fluids that may have precipitated phlogopite.

Glass. Hunter and Taylor (1982) reported glass in garnet kelyphytic rims from the kimberlite of Fayette County (Pennsylvania) with a similar composition to those from Udachnaya eclogites (Na-K enriched; Table 5). They suggested that such phases represent quenching during the final stages of kimberlite ascent through the upper mantle and lower crust. The difference in composition between garnet and glasses was interpreted as resulting from the incongruent melting of garnet. A similar process could have taken place during metasomatism of the Udachnaya eclogites. The presence of glass in garnet alteration rims in eclogites 5/91 and 51/3 may indicate that metasomatism of the Udachnaya eclogites occurred shortly before kimberlite eruption, and was probably related in some way to the host kimberlites. The metasomatizing agents could have their origin in the host kimberlite (e.g., Taylor and Neal, 1989) or may have infiltrated from the upper mantle as proposed by Hunter and Taylor (1982).

Serpentine. Despite the fact that the studied eclogites come from a single location (Udachnaya kimberlite pipe), they differ from each other in petrography, mineral chemistry, etc. The subdivision of the eclogites into two groups based on their petrography and mineral chemistry (after Cole-

man et al., 1965; Shervais et al., 1988; Taylor and Neal, 1989; Neal et al., 1990) is not reflected in the major- and trace-element composition of their alteration mineral assemblages. However, Group A eclogites (25/84 and 281/84) are distinctive from their B/C counterparts in that they contain *only* serpentine as a secondary mineral. These eclogites (Group A) were suggested to be transitional samples between eclogites and peridotites (Sobolev et al., 1994a; Snyder et al., 1997a), and therefore may have contained olivine (which has since completely altered to serpentine) in addition to the characteristic garnet-clinopyroxene eclogite mineral assemblage. In fact, olivine is recorded as a minor mineral in some eclogites (Dawson, 1980), and was reported in Group A eclogites from South Africa (Taylor and Neal, 1989; Pyle, 1995) and from Obnazhennaya, Siberia (Qi et al., 1994). Serpentines from eclogites 25/84 and 281/84 possess high Mg#'s (94 to 95), which may be a result of Mg enrichment and Fe depletion during metasomatism.

Discussion

Numerous studies have concentrated on studying secondary phases in mantle xenoliths, variations in compositions in primary phases, and textural relationships between constituent minerals (e.g., Aoki, 1975; Gurney et al., 1975; Harte and Gurney, 1975; Dawson and Smith, 1977; Erlank and Rickard, 1977; Haggerty et al., 1983; Erlank et al., 1987; Griffin et al., 1988; O'Reilly and Griffin, 1988; Hawksworth et al., 1990; Dautria et al., 1992; Rudnick et al., 1992; Hoal et al., 1994). The vast majority of previous studies dealt with peridotites, since they are the most abundant among mantle xenoliths. Because of the fact that the typical primary peridotite mineral assemblage (1) consists of at least four minerals (i.e., olivine, clino- and orthopyroxene, garnet, and/or spinel) and (2) some of these minerals almost always possess intramineral compositional variations, it is impossible to calculate the primary whole-rock composition. Therefore, no attempt has been made to fully quantify metasomatic effects. Eclogites from Udachnaya are bimineralic rocks that exhibit little or no intramineral compositional variations. This study is a first attempt to quantify metasomatic overprinting, i.e., the amount and possible nature of metasomatic fluids that affected eclogites from Udachnaya.

Fraracci (1994) developed a geochemical mixing model using both major and trace elements in order to evaluate the influence of kimberlitic metasomatism on eclogites from the Mir kimberlite. It was demonstrated that the proportion of mixing with kimberlite magma varied for each element within a single sample. According to Fraracci (1994), Mir eclogites possess a common source of metasomatism, with significant contribution from the host kimberlitic magma. However, it is unclear whether so-called "kimberlitic" fluids in equilibrium with the silicate magma should retain the *general* chemical composition of the kimberlite magma. Eggler (1987) stated that partition coefficients between an H_2O-CO_2 fluid and silicate melt are approximately 0.01 (P = 5 to 10 kbar) for most of the major elements, and are in the range of 10 to 30 (P = 20 to 40 kbar) for the REE. According to Eggler (1987), partition coefficients for the major elements increase with pressure and approach 0.5 at P = 20 to 25 kbar. Kimberlite chemical analyses demonstrate the presence of 5 to 17 wt% CO_2 (Vasilenko, 1995), and therefore, fluids associated with kimberlitic magma probably contain significant amounts of CO_2. Calcite, which is present in 6 of the 10 studied eclogites (Table 1), can be the result of the interaction of these eclogites with such fluids. These 6 samples also contain H_2O-bearing phases (amphibole, phlogopite, serpentine), which means that the fluid(s) undoubtedly contains H_2O as well.

Composition of metasomatic fluid (elemental ratios and major elements)

In order to evaluate whether kimberlite was the source for the metasomatic fluid, ratios of various elements for C^i_{WR} and C_{MWR} were compared to kimberlite ratios (Fig. 5). All possible ratio combinations were tested; Figure 5 represents those with the most consistent changes (i.e., tie lines being parallel or pointing in the same directions) from C^i_{WR} to C_{MWR}. The fluid composition (assuming one source for the eclogites) should lie on an extension of the tie lines (i.e., $C^i_{WR} \rightarrow C_{MWR} \rightarrow C_{M}$). For certain ratios, the metasomatic source is similar, if not the same, for all eclogites, which is shown by tie lines connecting C_{MWR} and C^i_{WR} values. In most cases, the fluid composition is quite similar to that of the kimberlite. Some samples do not fall into the overall picture (e.g., 35/1 on CaO/MgO versus La/MgO plot and 1/79

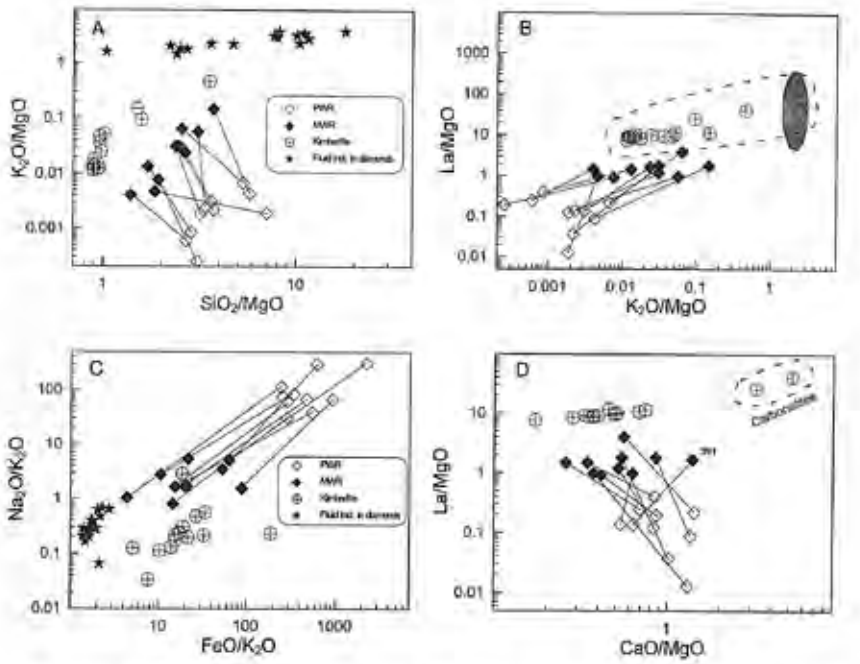

FIG. 5. Various ratios for C_{fPWR}, C_{fMWR}, Udachnaya kimberlite, and fluid inclusions in African diamonds (data from Schrauder and Navon, 1994). Shaded field on K_2O/MgO versus La/MgO plot represents fluid composition. REE abundances are normalized.

on K_2O/MgO versus La/MgO plot) and may be a result of a different style of metasomatism. It also is possible that some of the eclogite alteration was overprinted by weathering, although it is likely that ratio plots with more randomly oriented tie lines (not shown) would be indicative of weathering, rather than metasomatism.

By connecting C_{fMWR} and C_{fPWR} compositions with tie lines, one can determine only the direction (i.e., the extension of a tie line) where the composition of the metasomatic fluid should plot. A representative sample of the mantle fluid is needed in order to speculate about the nature of "eclogite" metasomatism. Fluid inclusions trapped in fibrous diamonds could represent such a sample. Schrauder and Navon (1994) reported that fluids trapped in African diamonds span a wide range between hydrous and carbonatitic end members, and they are widespread in the subcontinental mantle. Schrauder et al. (1994) demonstrated that fluid inclusions from Yakutian diamonds extend the range of compositions and span a wide range in SiO_2 contents (9 to 70 wt%), as well as in CaO and MgO (5 to 32 and 3 to 28 wt%, respectively). These fluid inclusions also are enriched in K_2O (up to 22.2 wt%), TiO_2 (4.2 to 5.1 wt%), and Cl (0.8 to 1.7 wt%). We have plotted chemical ratios for fluid inclusions in diamonds (data from Schrauder and Navon, 1994), which are shown in Figures 5A and 5C, along with C_{fPWR}, C_{fMWR}, and kimberlite ratios. It is clear that the compositions of the fluids trapped in diamonds lie along the extension of tie lines for the Udachnaya eclogites. If diamonds are metasomatic in origin (Taylor et al., 1998), then these fluids could represent a hypothetical metasomatic agent. Conversely, fluids may have had their origin from the host kimberlite, which also is illustrated in Figure 5. It is obvious that not all elemental ratios are consistent with a single

metasomatic agent (e.g., CaO/MgO). In fact, an extension of the tie line of sample 35/1 points to Udachnaya carbonatites (Fig. 5D).

The approach described above helps to reveal similarity or dissimilarity of the metasomatic fluid to known mantle fluid compositions. However, this approach may be oversimplified and represents a general "mixing" model that may not work for the metasomatism of Udachnaya eclogites. All eclogites are enriched in MgO compared to $C_{i\text{-}WR}$ values, and yet fluid compositions from diamond inclusions do not exceed 10.9 wt% MgO (Schrauder and Navon, 1994). Relative Δ_m^{MgO} values from Table 5 are >100% for some samples, which indicates a metasomatic source rich in Mg. This may be explained by a difference in partition coefficients for Mg between eclogitic melt and metasomatic fluid. It is clear that $D_{Mg}^{fluid/melt}$ for metasomatic fluids is less than 1, and should be in the range of 0.1 to 0.01. However, in order to dissolve 10.9 wt% MgO with such a low partition coefficient, the fluid must have originated at 200 to 400 km depth, as suggested for an aqueous vapor-phase coexisting with peridotite (Wyllie, 1995). Although it is impossible to determine the fluid composition in terms of absolute elemental abundances, ratios of elements can be estimated. Assuming MgO contents in the fluid similar to those determined by Schrauder and Navon (1994), we plotted a metasomatic fluid field on Figure 5B (K_2O/MgO versus La/MgO). The La concentration in this fluid, calculated from the La/MgO ratio, could be as high as 1500 to 2000 ppm La. This was calculated using MgO contents of 3.3 (hydrous end member) and 13.3 wt% (carbonatitic end member) for fluids trapped in diamonds (Schrauder and Navon, 1994). It is clear that this hypothetical metasomatic fluid (Fig. 5B) is quite similar to kimberlite in composition, lying on the extension of the kimberlite-carbonatite trend. This suggests that some fluids that affected Udachnaya eclogites may have been enriched in K, therefore having a K_2O/MgO ratio higher than that of kimberlites.

Composition of metasomatic fluid (rare-earth element)

It has been demonstrated that metasomatized rocks are enriched in incompatible and LIL (large-ion lithophile) elements (e.g., Dawson, 1984; Erlank et al., 1987; Hawkesworth et al., 1990; Rudnick et al., 1993). Therefore, it is no surprise that all $C_{i\text{-}AWR}$ (altered whole-rock compositions) show enrichment in LREE when compared to $C_{i\text{-}UWR}$ (Fig. 4). The degree of enrichment between the REE, however, is significantly different. This may be caused by a number of factors, such as: (1) the garnet: clinopyroxene ratio, which varies from sample to sample; (2) duration of the metasomatic event, which also may vary for different samples; and (3) differences in whole-rock chemical compositions. Based on REE patterns for AWR and CWR we suggest that, for at least the LREE, the metasomatic source was similar in composition for all eclogites. The Udachnaya kimberlite (Tables 6 and 7; Fig. 4) is similar in LREE and MREE composition to this metasomatic source but is different in HREE.

Schrauder and Koeberl (1994) determined REE contents in fluid inclusions from African fibrous diamonds and found that LREE values are significantly different from those of most kimberlites. According to these authors, La concentrations decrease from 600 ppm in the carbonatitic end member to 300 ppm in the hydrous end member. They also stated that the La/Yb ratio in the fluid is lower than that in carbonatites and kimberlites, whereas the REE patterns are steeper. La values for both carbonatitic and hydrous end members significantly exceed those of the Udachnaya kimberlite (600 and 300 ppm, respectively, versus 63 ppm). Although these values are not as large as calculated from the La/MgO ratio (1500 to 2000 ppm; see above), they exceed those of the Udachnaya kimberlite by an order of magnitude. This suggests that the REE contents of the metasomatic fluid(s), although similar in general (pattern shape), are different from those of kimberlite.

A "kimberlitic" fluid, however, may have played a significant role in formation of some secondary minerals, and therefore, overall metasomatic enrichment/depletion of the eclogites. Based on measured phlogopite $^{143}Nd/^{144}Nd$ and $^{147}Sm/^{144}Nd$ ratios (Snyder et al., 1997), we determined a "metasomatic" model age for samples 41/3 and 108/3. The model age is 550 Ma for 41/3, and 480 Ma for 108/3, which is similar to the age of Udachnaya kimberlite (367 Ma; Kinny et al., 1997) and suggests that phlogopite was formed relatively recently, possibly during late kimberlitic metasomatism. Nevertheless, this does not rule out earlier, mantle metasomatic events for other phases.

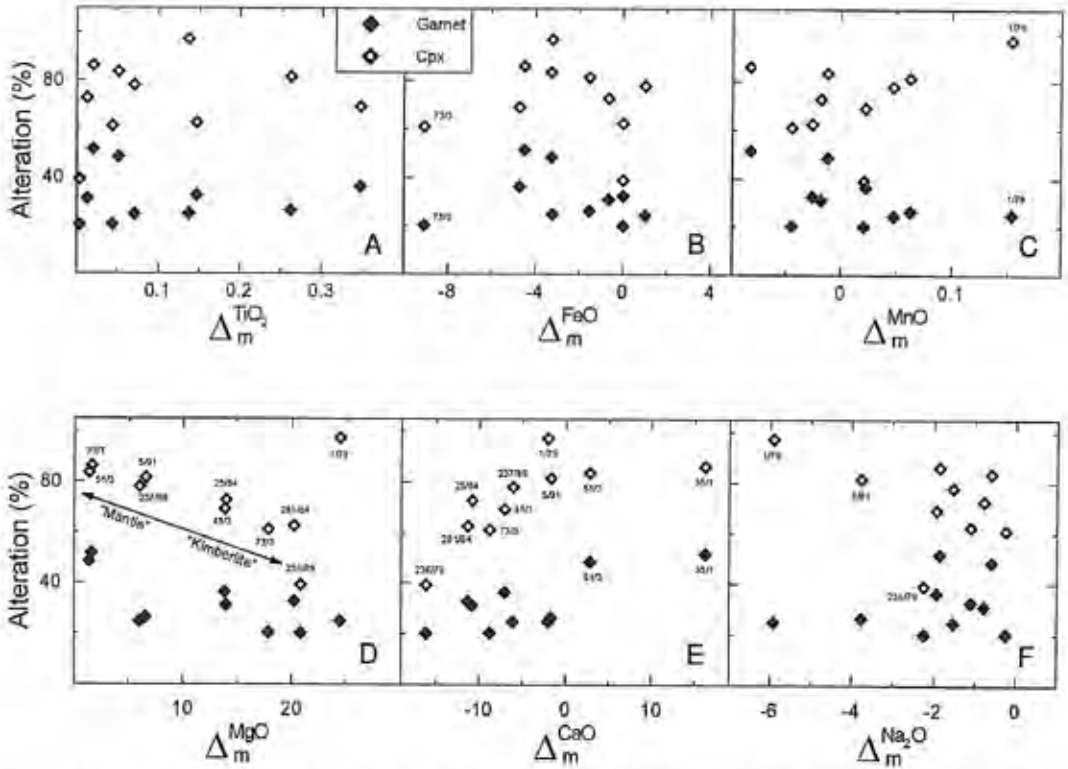

FIG. 6. Garnet and clinopyroxene alteration versus absolute Δ'_m values. The line dividing plots B, C, and E corresponds to $\Delta'_m = 0$, and any trend split by this line should be viewed as two separate trends (depletion trend on the left-hand side, and enrichment on the right).

TABLE 6. Major-Element Analyses of Udachnaya Kimberlites and Carbonatites

N of samples:	12	13	26	41	42	49	56	70	82	90	96
SiO_2	16.3	25.8	27.4	28.1	26.5	23.5	28.2	26.4	26.1	28.4	27.5
TiO_2	0.58	1.07	1.24	1.41	1.09	0.80	1.12	1.47	1.15	1.00	1.00
Al_2O_3	2.62	2.40	1.98	2.00	1.57	2.36	1.73	2.18	1.91	1.85	2.68
FeO	1.75	6.93	7.45	8.38	7.71	4.06	5.86	6.80	7.24	4.91	6.85
MgO	10.3	26.5	30.7	31.8	29.9	23.3	29.8	27.5	29.8	25.2	30.5
CaO	33.0	13.5	10.7	8.99	11.0	17.3	11.2	13.4	11.7	17.1	11.3
Na_2O	0.12	1.46	0.09	0.11	0.11	0.04	0.09	0.13	0.10	0.08	0.09
K_2O	0.96	0.65	0.39	0.56	0.36	1.20	0.37	0.99	0.42	0.37	0.42
P_2O_5	0.34	0.34	0.01	0.39	0.41	0.53	0.35	0.49	0.42	0.32	0.21
LOI	33.8	20.5	19.4	17.3	20.3	26.1	20.9	20.2	20.5	25.4	18.9
Total	99.77	99.23	99.37	99.40	99.73	99.23	99.63	99.54	99.41	99.64	99.44

Source: Vasilenko, 1995.

TABLE 7. REE Analyses of Udachnaya Kimberlites and Carbonatites

Sample:	U-1a	U-1b
La	58.2	66.3
Ce	105.5	122.7
Pr	9.56	11.3
Nd	33.9	39.9
Sm	4.60	5.52
Eu	1.21	1.37
Gd	3.56	4.01
Tb	0.30	0.33
Dy	1.59	1.82
Ho	0.26	0.27
Er	0.59	0.67
Tm	0.07	0.12
Yb	0.43	0.44
Lu	0.06	0.06

Source: This study.

Metasomatic models

Figure 6 shows the proportion of garnet and clinopyroxene alteration versus Δ^{t}_{m} values for several elements. There is no correlation between $\Delta^{TiO_2}_{m}$ and alteration (Fig. 6A), which could be a result of low modal abundance of Ti-bearing secondary phases. Little correlation is present in Figure 6B, although there is a slight increase of degree of alteration with depletion in FeO (except for sample 73/3, Fig. 6B). There is a positive (note that the X axis is negative in Fig. 6E) correlation between Δ^{CaO}_{m} and clinopyroxene alteration (depletion in Ca), although two samples (35/1 and 51/3) are enriched in CaO. These samples may have been affected by carbonatite-like metasomatism, which resulted in their enrichment in Ca when compared to other Udachnaya eclogites. As stated by Rudnick et al. (1993), carbonatite-melt metasomatism is characterized by enrichment of only the major element Ca, whereas the silicate-melt metasomatism "signature" is an enrichment in Fe, Al, Ca, and Ti (Irving, 1980; Wilshire et al., 1980; Rudnick et al., 1993). However, according to Rudnick et al., an initial carbonatite melt has low (~30) Ti/Eu and high Ca/Al (60 to 70) ratios, whereas hypothetical metasomatic fluids for the Udachnaya eclogites (35/1 and 51/3) yield distinctly different values: 2000 to 5000 for Ti/Eu and ~10 for Ca/Al. Hence, it is possible that the metasomatic agent that affected the eclogites was either not homogeneous, or some "local" metasomatic event has taken place in addition to the major one.

The negative correlation (Fig. 6D) between mineral alteration and Δ^{MgO}_{m} is highly unusual. It means that the *most altered* samples are *less enriched* in Mg (Fig. 6D) and *less depleted* in Ca (Fig. 6F). Based on these observations, we suggest that the trend in Figure 6D (with the exception of sample 1/79) may represent both "kimberlite" and "mantle" metasomatism for the Udachnaya eclogites. Xenoliths at the "kimberlite" end were affected by metasomatic fluids with relatively high MgO contents, whereas those at the "mantle" end (e.g., 35/ and 51/3) were affected by fluids with lower MgO for a much longer period of time. These two "mantle" samples also are the only xenoliths having positive Δ^{CaO}_{m}.

The aforementioned observations, combined with the general enrichment/depletion patterns, suggest that the Udachnaya eclogites were affected by similar (but not the same) types of metasomatic fluids. Despite some differences, the fluids also were similar in some respects to that of kimberlite. They were enriched in Mg, Ti, K, Cl, F, H_2O, and LREE and depleted in Si, Al, and Fe, which is in good agreement with Udachnaya peridotites, with the exception of Fe (Boyd et al., 1997).

The eclogites could have resided at various depths in the upper mantle, where metasomatic fluids of slightly different composition were passing through. Although different in composition, it is not clear whether they affected the eclogites at different times. These "metasomatites" are similar to kimberlites in general patterns (e.g., K, Mg, Ti, REE enrichment) and different at the same time in the abundances of these elements.

Summary

1. Udachnaya eclogites represent a unique suite of samples that are chemically homogeneous and represent an important test case for modal metasomatism. This metasomatism resulted in the appearance of numerous secondary phases (i.e., typical metasomatic minerals such as phlogopite, amphibole, djerfisherite, sodalite, etc.) in the eclogites without significant trace-element enrichment of the primary minerals. Similarities in metasomatic patterns (Δ^i_m) for major and trace elements, and correlation between different Δ^i_m values, suggest that Udachnaya eclogites were exposed to one major metasomatic event, with consequent or simultaneous metasomatism by more localized fluids.

2. The major metasomatic source was similar to kimberlite in general enrichment/depletion patterns, but different in composition in terms of major- and trace-element abundances. The fluids were more enriched in TiO_2, K_2O, Cl, FeO, and LREE (up to 300–600 ppm of La) than is the case for kimberlites. These fluids were CO_2-H_2O enriched and contained significant amounts of Cl and F. They enriched the eclogites in MgO, TiO_2, K_2O, and LREE, and depleted them in SiO_2, Na_2O, and FeO. A mantle-derived carbonatite-like fluid affected samples 35/2 and 51/3, and resulted in much higher Ca contents of measured whole-rock values for these samples when compared to the other eclogites.

3. Group A eclogites are significantly different from the other samples not only in their major-element chemistry of primary minerals and petrography, but also in their secondary-mineral assemblages, containing only serpentine as a secondary mineral. This may indicate the presence of olivine in these rocks prior to metasomatism.

4. A simple mixing model fails to explain all metasomatic patterns of Udachnaya eclogites. Although a "primary" metasomatic overprint may be somewhat masked by weathering, and may have involved later localized fluids, its major contribution can be revealed using a quantitative approach. It is shown that the inferred metasomatic agent represents the case of "truly" mantle metasomatism and is different in timing and composition from the host kimberlite. Based on fluid/melt major-element partition coefficients, this metasomatic fluid may have originated at depths of 200 to 400 km.

Acknowledgments

The authors wish to thank Allan Patchen for assistance with the electron-microprobe analyses. INA analyses for eclogites were performed at the High Flux Isotope Reactor (HFIR) facility at the Oak Ridge National Laboratory (ORNL). ICPMS analyses for kimberlites were performed at the University of Notre Dame. The research for this paper was partially supported by NSF Grant EAR-93-04053, for which we are grateful. The authors also wish to thank Dmitri Ionov and another anonymous reviewer for reviewing an earlier version of the manuscript. Constructive comments by Igor Ryabchikov and Lia Kogarko have greatly improved the manuscript.

REFERENCES

Aoki, K., 1975, Origin of phlogopite and potassic richterite-bearing peridotite xenoliths from South Africa: Contrib. Mineral Petrol. v. 53, p. 145–156.

Ayers, J. C., and Eggler, D. H., 1995, Partitioning of elements between silicate melt and H_2O-NaCl fluids at 1.5 and 2.0 Gpa pressure: Implications for mantle metasomatism: Geochim. et Cosmochim. Acta, v. 59, p. 4237–4246.

Baedecker, P. A., and Grossman, J. N., 1969, The computer analysis of high resolution gamma-ray spectra from instrumental activation analysis experiments: U.S. Geol. Surv. report.

Beard, B. L., Fraracci, K. N., Taylor, L. A., Snyder, G. A., Clayton, R. N., Mayeda, T. K., and Sobolev, N. V., 1996, Petrography and geochemistry of eclogites from the Mir kimberlite, Russia: Contrib. Mineral. Petrol., v. 125, p. 293–310.

Boyd, F. R., Pokhilenko, N. P., Pearson, D. G., Mertzman, S. A., Sobolev, N. V., and Finger, L. W., 1997, Composition of the Siberian cratonic mantle: Evidence from Udachnaya peridotite xenoliths: Contrib. Mineral. Petrol., v. 128, nos. 2/3, p. 228–246.

Brenan, J. M., 1993, Partitioning of fluorine and chlorine between apatite and aqueous fluids at high pressure and temperature: Implications for the F and Cl content of high P-T fluids: Earth Planet Sci. Lett., v. 117, p. 251–263.

Bulanova, G. P., Shestakova, O. E., and Leskova, N. V., 1982, Sulfide inclusions in diamonds: Zapiski Vsesoyuznogo Mineralogicheskogo Obshchestva, v. 111, no. 5, p. 557–562 (in Russian).

Coleman, R. G., Lee, D. E., Beatty, L. B., and Brannock, W. W., 1965, Eclogites and eclogites: Their differences and similarities: Bull. Geol. Soc. Amer., v. 76, p. 483–508.

Dautria, J. M., Dupuy, C., Takherist, D., and Dostal, J., 1992, Carbonate metasomatism in the lithospheric mantle: Peridotitic xenoliths from a melilitic district of the Sahara basin: Contrib. Mineral. Petrol., v. 111, p. 37–52.

Dawson, J. B., 1980, Kimberlites and their xenoliths: Berlin, Springer-Verlag, p. 148–183.

———, 1984, Contrasting types of upper mantle metasomatism, in Kornprobst, J., ed., Kimberlites II: The mantle and crust-mantle relationships: Amsterdam, Elsevier, p. 289–294.

Dawson, J. B., and Smith, J. V., 1975, Chemistry and origin of phlogopite megacrysts in kimberlite: Nature, v. 253, p. 336–338.

———, 1977, The MARID (mica-amphibole-rutile-ilmenite-diopside) suite of xenoliths in kimberlite: Geochimet. Cosmochim. Acta, v. 41, p. 309–323.

Donaldson, C. H., 1978, Petrology of the upper-most mantle deduced from spinel lherzolite nodules at Caton Hill, Derbyshire: Contrib. Mineral. Petrol., v. 65, p. 363–377.

Deer, W. A., Howie, R. A., and Zussman, J., 1992, An introduction to the rock-forming minerals: New York, Longman, esp. p. 192–195.

Eggler, D. H., 1987, Solubility of major and trace elements in mantle metasomatic fluids: Experimental constraints, in Menzies, M. A., and Hawkesworth, C. J., eds, Mantle metasomatism: London, Academic Press, p. 21–44.

Erlank, A. J., and Rickard, R. S., 1977, Potassic richterite-bearing peridotites from kimberlite and the evidence they provide for upper-mantle metasomatism [abs.]: Ext. Abs. 2nd Int. Kimb. Conf., Santa Fe, NM, unpaginated.

Erlank, A. J., Waters, F. G., Hawkesworth, C. J., Haggerty, S. E., Allsop, H. L., Rickard, R. S., and Menzies, M. A., 1987, Evidence for mantle metasomatism in peridotite nodules from the Kimberley pipes, South Africa, in Menzies, M. A., and Hawkesworth, C. J., eds., Mantle metasomatism: London, Academic Press, p. 221–309.

Fraracci, K. N., 1994, Diamondiferous eclogite xenoliths from the Mir kimberlite, Yakutia, Siberia: Geochemistry, and petrogenesis: Unpubl. M. S., thesis, University of Tennessee, Knoxville.

Godovikov, A. A., 1983, Mineralogy: Novosibirsk, Nauka Press, 648 p. (in Russian).

Gavorov, I. N., Blagulaveva, N. S., Kiyukhina, N. I., Kharkiv, A. D., and Shcheglov, A. D., 1984, Primary potassium minerals in deep-seated eclogites of Yakutia: Int. Geol. Rev., v. 26, p. 1290–1294.

Griffin, W. L., O'Reilly, S. Y., and Stabel, T., 1988, Mantle metasomatism beneath western Victoria Australia: II. Isotopic geochemistry of Cr diopside lherzolites and Al-augite pyroxenites: Geochim. et Cosmochim. Acta, v. 52, p. 449–459.

Gurney, J. J., Dawson, J. B., Harte, B., and Lawless P. J., 1975, The bulk chemical composition of peridotite facies rocks from the Matsoku and Bulfontein pipes [abs.]: Ext. Abs. Kimb. Symp., Cambridge, p. 3–5.

Haggerty, S. E., Smyth, J. R., Erlank, A. J., Rickard, R. S., and Danchin, R. V., 1983, Lindsleyite (Ba) and mathiasite (K): Two new chromium titanates in the crichtonite series from the upper mantle: Amer. Mineral., v. 68, p. 494–505.

Harte, B., and Gurney, J. J., 1975, Ore mineral and phlogopite mineralization within ultramafic nodules from the Matsoku kimberlite pipe, Lesotho: Carnegie Inst. Wash. Yearbook, v. 74, p. 528–536.

Hawkesworth, C. J., Erlank, A. J., Kempton, P. D., and Waters, F. G., 1990, Mantle metasomatism: Isotope and trace-element trends in xenoliths from Kimberley, South Africa: Chem. Geol., v. 85, p. 19–34.

Hoal, K. E. O., Hoal, B. G., Erlank, A. J., and Shimizu, N., 1994, Metasomatism of the mantle lithosphere recorded by rare elements in garnets: Earth Planet Sci. Lett., v. 126, p. 303–313.

Hunter, R. H., and Taylor, L. A., 1982, Instability of garnet from the mantle: Glass as evidence of metasomatic melting: Geology, v. 10, p. 617–620.

Irving, A. J., 1980, Petrology and geochemistry of composite ultramafic xenoliths in alkalic basalts and implications for magmatic processes within the mantle: Amer. Jour. Sci., v. 280A, p. 389–426.

Jerde, E. A., Taylor, L. A., Crozaz, G., Sobolev, N. V., and Sobolev, V. N., 1993, Diamondiferous eclogites from Yakutia, Siberia: Evidence for a diversity of protoliths: Contrib. Mineral. Petrol., v. 114, p. 189–202.

Jezek, P. A., Sinton, J. M., Jamsewicki, E., and Obermeyer, C. R., 1978, Fusion of rock and mineral powders for

electron microprobe analysis: Smithson. Contrib. Earth Sci., v. 22, p. 46–52.

Jin, Y., and Taylor, L. A., 1987, Compositional variations in the upper mantle spinel peridotite facies beneath Eastern China [abs.]: EOS (Trans. Amer. Geophys. Union), v. 68, p. 1552.

Jones, A. P., Smith, J. V., and Dawson, J. B., 1982, Mantle metasomatism in 14 veined peridotites from Bultfontein mine, South Africa: Jour. Geol., v. 90, p. 435–453.

Kimberlites of Yakutia: Field guide book, 1995, Novosibirsk, 108 p.

Kinny, P. D., Griffin, B. L., Heaman, L. M., Brakhfogel, F. F., and Spetsius, Z. V., 1997, SHRIMP U-Pb ages of perovskite from Yakutian kimberlites: Russ. Geol. Geophys., v. 38, p. 97–105.

Kramers, J., Ruddick, J., and Dawson, J. B., 1983, Trace element and isotope studies of veined, metasomatic and 'MARID' xenoliths from Bultfontein South Africa: Earth Planet Sci. Lett., v. 65, p. 90–106.

Lundberg, L. L., Crozaz, G., McKay, G., and Zinner, E., 1988, Rare earth element carriers in the Shergotty meteorite and implications for its chronology: Geochim. et Cosmochim. Acta, v. 52, p. 2147–2163.

Lundberg, L. L., Crozaz, G., and McSween, H. Y., Jr., 1990, Rare earth elements in minerals of the ALHA77005 shergottite and implications for its parent magma and crystallization history: Geochim. et Cosmochim. Acta, v. 54, p. 2535–2547.

Neal, C. R., Taylor, L. A., Davidson, J. P., Holden, P., Halliday, A. N., Nixon, P. H., Paces, J. B., Clayton, R. N., and Mayeda, T. K., 1990, Eclogites with oceanic crustal and mantle signatures from the Bellsbank kimberlite, South Africa, part 2: Sr, Nd, and O isotope geochemistry: Earth Planet Sci. Lett., v. 99, p. 362–379.

O'Reilly, S. Y., and Griffin, W. L., 1988, Mantle metasomatism beneath western Victoria Australia: I. Metasomatic processes in Cr diopside lherzolites: Geochim. et Cosmochim. Acta, v. 52, p. 433–448.

Pyle, J. M., 1995, The petrography, mineral chemistry, and geochemistry of upper mantle eclogites, Jagersfontein kimberlite, South Africa: Unpubl. M. S. thesis, University of Massachusetts.

Rudnick, R. L., McDonough, W. F., and Chappell, B. W., 1993, Carbonatite metasomatism in the northern Tanzanian mantle: Petrographic and geochemical characteristics: Earth Planet Sci. Lett., v. 114, p. 463–475.

Ryabchikov, I. D., 1993, Fluid transport of ore metals in ultramafic mantle rocks: Proc. 8th Quad. IAGOD Symp., Schweiz. Verlag., p. 425–433.

Ryabchikov, I. D., Schreyer, W., and Abraham, K., 1982, Compositions of aqueous fluids in equilibrium with pyroxenes and olivines at mantle pressures and temperatures: Contrib. Mineral Petrol., v. 79, p. 80–84.

Qi, Q., Taylor, L. A., Snyder, G. A., and Sobolev, N. V., 1994, Eclogites from the Obnazhennya kimberlite pipe, Yakutia, Russia: Int. Geol. Rev., v. 36, p. 911–924.

Schrauder, M., and Koeberl, C., 1994, Trace element analyses of fluid-bearing fibrous diamonds from Jwaneng (Botswana) by neutron activation analysis: Mineral Mag., v. 58A, p. 811–812.

Schrauder, M., and Navon, O., 1994, Hydrous and carbonatitic mantle fluids in fibrous diamonds from Jwaneng, Botswana: Geochim. et Cosmochim. Acta., v. 58, p. 761–771.

Schrauder, M., Navon, O., Szafranek, D., Kaminsky, F. V., and Galimov, E. M., 1994, Fluids in Yakutian and Indian diamonds: Mineral. Mag., v. 58A, p. 813–814.

Schuraytz, B. C., and Ryder, G. 1990, An evaluation of the reliability and usefulness of microprobe fused bead analyses for petrogenetic interpretations [abs.]: Abs., 21st Lunar Planet Sci. Conf., p. 1113–1114.

Shervais, J. W., Taylor, L. A., Lugmair, G. W., Clayton, R. N., Mayeda, T. K., and Korotev, R. L., 1988, Early Proterozoic oceanic crust and the evolution of subcontinental mantle: Eclogites and related rocks from southern Africa: Geol. Soc. Amer. Bull., v. 100, p. 411–423.

Snyder, G. A., Taylor, L. A., Crozaz, G., Halliday, A. N., Beard, B. L., Sobolev, V. N., and Sobolev, N. V., 1997a, The origins of Yakutian eclogite xenoliths: Jour. Petrol., v. 38, p. 85–113.

Snyder, G. A., Taylor, L. A., Taylor, D. H., and Jin, Y., 1997b, Mantle lherzolite xenoliths from Eastern China: Textures of secondary minerals: Int. Geol. Rev., v. 39, p. 671–687.

Sobolev, V. N., 1997, Mantle metasomatism beneath the Siberian Platform: Unpubl. PhD. dissertation, University of Tennessee, Knoxville.

Sobolev, V. N., Taylor, L. A., Snyder, G. A., and Sobolev, N. V., 1994a, Diamondiferous eclogites from the Siberian Platform: Samples with peridotitic signatures: EOS (Trans. Amer. Geophys. Union), v. 75, p. 192.

———, 1994b, Diamondiferous eclogites from the Udachnaya kimberlite pipe, Yakutia, Siberia: Int. Geol. Rev., v. 36, p. 42–64.

Spetsius, Z. V., Bulanova, G. P., and Leskova, N. V., 1985, Djerfisherite and its genesis in kimberlitic rocks: Dokl. Akad. Nauk SSSR, v. 293, p. 199–202.

Taylor, L. A., Milledge, H. J., Bulanova, G. P., Snyder, G. A., and Keller, R. A., 1998, Metasomatic eclogitic diamond growth: Evidence from multiple diamond inclusions: Int. Geol. Rev., v. 40, p. 663–676.

Taylor, L. A., and Neal, C. R., 1989, Eclogites with oceanic crustal and mantle signatures from the Bellsbank kimberlite, South Africa, part I: Mineralogy, petrography, and whole rock chemistry: Jour. Geol., v. 97, p. 551–567.

Taylor, L. A., Snyder, G. A., Crozaz, G., Sobolev, V. N., Yefimova, E. S., and Sobolev, V., 1996, Eclogitic inclusions in diamonds: Evidence of complex mantle

processes over time: Earth Planet Sci. Lett., v. 142, p. 535–551.
Vasilenko, V. B., 1995, Petrochemistry of the major diamond deposits of Yakutia, *in* Sobolev, N. V., Zuyev, V. M., Afanas'yev, V. P., Pokhilenko, N. P., and Zinchuk, N. N., eds., Kimberlites of Yakutia: Novosibirsk, United Institute of Geology, Geophysics and Mineralogy, p. 46–60.
Wilshire, H. G., Nielson Pike, J. E., Meyer, C. E., and Schwarzman, E. C., 1980, Amphibole-rich veins in lherzolitic xenoliths: Dish Hill and Deadman Lake, California: Amer. Jour. Sci., v. 280-A, p. 576–593.
Wyllie, P. J., 1995, Experimental petrology of upper mantle materials, processes and products: Jour. Geodynam., v. 20, p. 429–468.
Zinner, E., and Crozaz, G., 1986, A method for the quantitative measurement of rare earth elements in the ion microprobe: Int. Jour. Mass Spectrom. Ion Proc., v. 69, p. 17–38.

Appendix: Methodology for Quantifying Metasomatism

Reconstructed whole-rock chemistry

The most representative thin sections from each sample were examined by point counting (≅1500 points per thin section). An attempt was made to reconstruct primary mineralogy using modes obtained by allocating the secondary alteration minerals to either garnet or clinopyroxene (e.g., a garnet alteration rim would be allocated to garnet). We also assume in the preceding discussion that all of the alteration is due to either kimberlitic or mantle-derived metasomatism and not to surface weathering. Because of relative freshness of these samples and the host kimberlite, this is a logical first approach. Many samples are coarse grained, with grain sizes up to 8–9 mm. Because of these grain sizes, and also because of the small sample sizes (<50 g for samples 35/1, 41/3, 51/3, and 73/3), true modes are difficult to obtain. The question of precision in both major and trace elements in whole-rock reconstructions will be addressed in the discussion.

Major-element and REE compositions measured in whole-rock samples for the Udachnaya eclogites are presented in Table 4. The major differences in whole-rock chemistry between Groups A and B-C eclogites, based on the classification of Coleman et al. (1965) are MgO and Cr_2O_3 contents. Samples 25/84 and 281/84 (Group A) are characterized by higher Cr_2O_3 (0.55 and 0.95 wt%, respectively) and MgO (24.3 and 26.0 wt%, respectively) contents when compared to other samples (0.03 to 0.15 wt% Cr_2O_3, and 12.3 to 20.4 wt% MgO; Table 4).

Major-element and REE compositions of primary minerals (i.e., garnet and clinopyroxene) were used for the determination of reconstructed whole-rock values using measured modes, which can be expressed by following equation:

$$C_{PWR} = \sum (X_i^{cpx} * M_{cpx} + X_i^{gt} * M_{gt}), \qquad (1)$$

where C_{PWR} is the primary whole-rock composition, X_i^{cpx} and X_i^{gt} are chemical compositions of clinopyroxene and garnet in terms of element *i*, and M_{cpx} and M_{gt} are reconstructed modes of these minerals in the rock. The reconstructed mode is calculated using the measured mode of each primary phase (point-counting) and the alteration mode of this phase (point-counting). For instance, the measured mode for an unaltered garnet in sample 5/91 is 31%, and 11% for its alteration (Table 1); similarly, the measured mode for clinopyroxene is 11%, and 47% for its alteration. Therefore, a reconstructed Gt:Cpx mode for sample 5/91 is 42:58 (Table 1). This reconstructed mode for each primary phase is then multiplied by each elemental abundance. The value for each element in each phase is added together, resulting in a whole-rock composition of a bimineralic *pristine* (primary) assemblage of garnet and clinopyroxene. The primary whole-rock composition ostensibly represents the xenolith before metasomatism affected it. Both measured and primary whole-rock compositions are shown in Table 4. By comparing measured whole-rock (MWR) and primary whole-rock (PWR) compositions, it is possible to obtain a general idea about metasomatism. A first-order observation is that there is a depletion in SiO_2 and Na_2O, and enrichment in MgO and K_2O in MWR when compared to PWR.

Equations derived for quantifying metasomatism

The simple formula $WR_{measured} - WR_{primitive}$ = metasomatism (Frarracci, 1994) may not accurately quantify the effects of metasomatism. In order to quantify the metasomatic effects for Udachnaya eclogites, we can define the change in chemistry using the following mass-balance equation:

$$C_{MWR}^i = C_{PWR}^i \times (1 - Y_i) + C_{MR}^i \times (Y_i), \qquad (2)$$

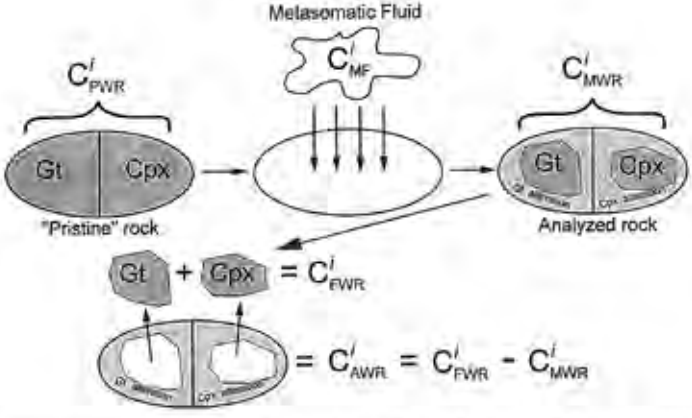

FIG. 7. Scheme of metasomatism for the Udachnaya eclogites. C^i_{PWR} is the primary whole-rock composition for each element; C^i_{MWR} is the measured (analyzed) whole-rock composition for this element; C^i_{MF} is the metasomatic whole-rock composition; C^i_{FWR} is the fresh whole-rock composition for each element (normalized modal % of unaltered garnet and clinopyroxene multiplied by composition of each mineral); and C^i_{AWR} is the altered whole-rock composition (calculated by subtracting C^i_{FWR} from C^i_{MWR}).

where C^i_{MWR} is the measured (analyzed) whole-rock composition for each element, C^i_{PWR} is the primary whole-rock composition for this element, C^i_{MF} is the composition of the element precipitated by metasomatic addition, and Y_i is the percentage mixing of primary whole-rock (C^i_{PWR}) with the metasomatic fluid (C^i_{MF}). By subtracting the pristine whole-rock composition (equation 1) from the measured whole-rock, we obtain some difference (Δ^i) for each element. However, this Δ^i includes not only the contribution from the metasomatic fluid, but also the contribution by the alteration of garnet and clinopyroxene. For instance, metasomatic phase A reacts with a mineral phase B, producing a secondary phase C (A + B = C), which incorporates both A and B (Fig. 7). We are interested only in composition of the metasomatic phase, and, therefore, in order to distinguish between contributions from metasomatism and primary minerals, the following equations were used:

$$C^i_{MWR} = C^i_{FWR} \times (1 - X) + C^i_{AWR} \times X, \quad (3)$$

and

$$C^i_{PWR} = C^i_{FWR} \times (1 - X) + C^i_{OWR} \times (X), \quad (4)$$

where C^i_{FWR} is the fresh whole-rock composition for each element (normalized modal % of unaltered garnet and clinopyroxene multiplied by composition of each mineral); C^i_{AWR} is the altered whole-rock composition (calculated by subtracting C^i_{FWR} from C^i_{MWR}), which includes both the fluid and primary-mineral contributions to the alteration; C^i_{OWR} is the contribution from the original garnet and clinopyroxene to the alteration; and X is the proportion of alteration. By subtracting C^i_{OWR} from C^i_{AWR} we obtain another delta (Δ^i_m), which is the numerical expression of the influence of the metasomatic fluid (C^i_{MF}). These values are shown in Table 5.